CHAPTER 4

Occurrence of arsenic and fluoride; and the associated hydrogeochemical processes: A comparative spatial and temporal distribution

4.1. Introduction

Arsenic in groundwater has been found to be a serious global concern. Majority of the people worldwide are reported to be dependent on groundwater for drinking, irrigation and other purposes. In Bangladesh and West Bengal, India; a switch from surface to groundwater has been observed since second half of the last century [1]. Inorganic As is toxic for consumption; high doses have been found to be outright fatal. Long term chronic exposure through drinking water reportedly leads to cancer, various degenerative effects of the circulatory system, and nervous system [2, 3]. Worldwide, the eastern parts of the Indian subcontinent, including Bangladesh and Indian parts of the Indo-Gangetic Plains especially West Bengal have been reported to be major hotspots of As contamination. Other countries found to be affected by groundwater As contamination are Vietnam, Cambodia, China, Nepal, Argentina, Chile, Mexico, United States etc [4- 14].

Recently As has also been reported from the North Eastern part of India including Assam [15]. High As and Fe were reported from the groundwaters of Tamarhat and Paglahat in Dhubri district, while the Charkola area in Bongaigaon has also reported high As levels exceeding the WHO [16] permissible limit of 10 μgL^{-1} [17], although no attempt was made to explore the hydrogeochemistry of the contamination. As was also reported in the groundwaters of Tripura, the study was conducted by the North East Regional Institute of Water and Land Management (NERIWALM), Tezpur, Assam, India. The Study reported As above 10 μgL^{-1} in 117 groundwater samples collected from different parts of Tripura [18], however like in the previous case, the hydrogeochemistry of the mechanism has not been explored. A similar study without an emphasis on the hydrogeochemistry was conducted in Dhakuakhana sub-division of

Lakhimpur district in Assam, India. It was found that As and Fe levels correlated and As was found in excess of 10 μgL^{-1} in the groundwater [19]. However none of these reports have delved deeper into the root of the problem i.e. the cause and the hydrogeochemistry affecting the distribution and mobilization of As in groundwater. In Assam, very high level of As was detected in Jorhat, Lakhimpur, Nalbari, and Nagaon districts. In the flood plain area of Assam, i.e. Barpeta, Dhemaji, Dhubri, Darrang, and Golaghat, arsenic was found in the range of 100-200 μgL^{-1} [20]. Out of the above mentioned districts, the highest level of groundwater As has been reported from the Jorhat district [18].

Reductive dissolution of Fe (III) oxyhydroxides has been reported to be the cause of high As in the groundwater of young Holocene aquifers by many workers/researchers [12, 13, 21- 26]. In addition abundance of organic matter in the newly deposited Holocene sediments have been found to induce microbial degradation of the former which consume O_2 and NO_3 [13, 21, 23, 27] creating a highly reductive environment.

Although we have discussed about the extent of groundwater As contamination around the world, but it is observed that As distribution is not uniform. In many regions where groundwater As has been detected and is a serious issue e.g., in the Middle Gangetic Plains (MGP) it is observed that As contamination is not continuous rather it occurs in patches. In case of MGP, entire districts or parts of districts like Ghazipur or Ballia are As effected but at the same time cities like Patna in Bihar which also lie in the MGP are reported to be free from groundwater As contamination. The same trend can be observed in other As effected regions around the world; even in the North Eastern part of India, the entire stretch of the BFP has not been found to be effected by As [18]. This shows that As mobilization is controlled by a number of factors like availability of As rich minerals, groundwater flow rates, age of sediments or local factors like use of anthropogenic phosphate fertilizers.

Another inorganic contaminant which has been proved to be a serious concern around groundwaters of the world is F^-. High concentrations of F^- (> 1.5 mgL^{-1}) in the groundwater have been found to be a major problem around the world [16, 28]. It has

been reported that around 25 million people around the world are suffering from high F^- related health disorders due to consumptions of F^- contaminated groundwater [28]. North and South America, Africa, the Middle Eastern countries, and India and China from Asia are reported to be some of the worst effected regions in this regard [29]. In India the problem of high groundwater F^- has been reported mainly from the southern and western states (Andhra Pradesh, Bihar, Gujarat, Madhya Pradesh, Punjab, Rajasthan, Tamil Nadu, and Uttar Pradesh) [28, 30]. Health effects related to high groundwater F^- like dental and skeletal fluorosis have been found to have a high prevalence in the above mentioned regions, and at present around 62 million people in India are reported to be at risk [28].

The North Eastern part of India including the state of Assam was unfortunately added to the list of the regions with high groundwater F^- in India in the last decade of the previous century [18]. In Assam very high groundwater F^- has been reported from the districts of Karbi Anglong and Nagaon [31, 32]. The situation in Karbi Anglong has been reported to be severe; around 646 people were identified with dental fluorosis and 36 with skeletal fluorosis way back in 2000 [32]. The number of effected people is expected to be much higher now. Recently the problem of high F^- groundwater has also been detected in urban areas like Guwahati, the largest city and the economic capital of Assam [33]. High F^- was detected in $NaHCO_3$ type groundwater from the Guwahati region [33]. Over all the number of works pertaining to F^- research in the North Eastern region of India including Assam has been found to be very low.

Fluoride mobilization in groundwater has been found to greatly depend on the rock type and the prevailing environmental conditions [29]. Fluoride has been found to accumulate during the process of "magmatic crystallization" and differentiation. In this regard crystalline rocks, especially "alkaline granites" which are deficient in Ca have been found to have high levels of F^- [29]. These rocks have been found to be abundant in the old Precambrian basement areas [29]. Sedimentary rocks also have been found to have quite high F^- levels; in such rocks F^- has been found to be present in the form of fluorite (CaF_2). Unconsolidated and clastic sediments have been found to contain even

higher amounts of F^- [29]. Metamorphic rocks have been found to have variable F^- content based on their source rocks [29].

Contact time has been found to be very important for F^- dissolution, as the primary mode of F^- mobilization is reported to be by mineral weathering and dissolution [29, 34, 35]. Therefore F^- has been found to occur mainly in arid to semi regions around the world where groundwater recharge rates are very low [28, 29, 36]. This observation has also been found to hold true in India, arid to semi arid environment has been found to be prevalent in the regions with high groundwater F^-. The average rainfall in the North Eastern region of India has been found to be very high, more over most of the northern part of Assam is found to be dominated by a fluvial environment due to the presence of the BFP. Thus the climatic and the environmental conditions in the state of Assam and rest of the North East India appear to be unsuitable for the occurrence of groundwater F^-. This could be one of the reasons for the localised occurrence of F^- in the BFP region of Assam.

The BFP is a vast region where population density has been found to be very high. A lot of uncertainty has been observed in the distribution of both As and F^- in the groundwater of this region. Moreover, as already stated, proper literature has been found to be lacking regarding the distribution and behaviour of groundwater As and F^- in the BFP. Therefore this chapter explores the distribution and the controls on groundwater As and F^- contamination in the BFP in the state of Assam with the following objectives: (i). Investigation of the spatial distribution of As and F^- in the BFP, (ii). Study of the impact of river proximity on As and F^- behaviour and, (iii). Understanding of the factors responsible for mobilization of As in the study area at the macro (BFP) and micro scale (Jorhat) levels. This chapter has been divided into three sections, the first section deals with the spatial and seasonal distribution and behaviour of As and F^- in the BFP. In the second section we discusses the influence of river proximity on As and F^- distribution. In the third section we discuss the As hydrogeochemistry in the Jorhat district.

4.2. Materials and methods

For the first section of this study, 40 groundwater samples were collected in both the pre-monsoon (February) and post-monsoon (September) seasons of 2011. Out of the 40 groundwater samples collected in each season, 13 samples were from the north bank and 27 samples from the south bank of the river Brahmaputra**.** While for the second, section 26 groundwater samples were collected in the monsoon season of 2013 (June) and 31 groundwater sample were collected in the post-monsoon season (January 2014) across the Jorhat district. Cation, anion, trace metal and DOC analyses were performed using the standard methods described in the chapter 2. Statistical analysis was performed using SPSS 20. Correlation analysis, hierarchical statistical analysis (HCA) and principal components analysis (PCA) were the statistical techniques used in this study. For mineralogical studies, 8 grab sediment samples were collected along the BFP. Contour mapping was utilized to observe the influence of river proximity on As and F^- distribution. Speciation modelling was done using the software MINTEQA2 v 3.1.

4.3. Results and discussion

4.3.1. Spatial and seasonal distribution of arsenic and fluoride in the Brahmaputra Flood Plains

4.3.1.1. Groundwater chemistry

Descriptive statistics of the groundwater parameters in both the north and south banks (spatial), and the pre and post-monsoon seasons (seasonal) have been presented in table 4.1 below.

Table 4.1: Descriptive statistics of the hydrochemical parameters spatially and seasonally, ND represents "not detectible"

Spatial variation								Seasonal variation					
North Bank					South Bank			Pre-monsoon			Post-monsoon		
Parameter	**Unit**	**Range**	**Mean**	**SD**	**Range**	**Mean**	**SD**	**Range**	**Mean**	**SD**	**Range**	**Mean**	**SD**
TDS	mgL^{-1}	21.50-783.00	186.94	158.58	29.90-345.00	139.14	75.96	21.5-375	137.	81.8	29.9-783	172	133
pH		5.31-8.10	6.79	0.77	5.04-10.12	6.96	0.94	5.04-7.24	6.29	0.54	6.18-10.2	7.53	0.71
ORP	mV	-135.70-(185.10)	2.32	63.32	-115.10-(140.60)	-6.59	48.81	-136-(-185)	5.8	60.1	-115-(-126)	-13.3	44.8
EC	µS/cm	43.40-1586.00	296.97	296.78	61.30-575.00	232.02	108.13	43.4-400	206	90.1	61.3-1586	299	246
Na^{+}	mgL^{-1}	3.40-35.00	16.68	11.85	0.96-41.50	13.33	8.40	3.4-38	12.3	7.93	0.96-41.5	16.6	11.07
K^{+}	mgL^{-1}	0.40-14.00	4.21	3.51	0.10-6.50	2.05	1.86	0.3-14	2.37	2.62	0.11-13.9	3.02	2.75
Ca^{2+}	mgL^{-1}	10.25-72.83	24.66	13.96	3.12-118.50	23.76	21.67	5.6-119	26.1	21.1	3.12-85	21.9	17.6
Mg^{2+}	mgL^{-1}	4.01-23.85	8.95	6.20	2.38-35.50	8.76	7.17	2.38-27.5	8.98	6.69	2.53-35.5	8.66	7.05
Cl^{-}	mgL^{-1}	5.68-332.28	44.46	61.89	5.68-71.00	25.56	16.00	5.68-88	25.8	17.7	5.68-332	37.5	50.8
SO_4^{2-}	mgL^{-1}	0.03-60.97	15.01	14.39	6.00-142.36	13.57	23.42	6.1-103	13.4	16.7	0.03-142	14.6	24.7
PO_4^{3-}	mgL^{-1}	0.22-1.83	0.42	0.35	0.16-2.56	0.47	0.44	0.16-1.83	0.52	0.4	0.16-2.56	0.39	0.42
NO_3^{-}	mgL^{-1}	ND-1.96	0.52	0.54	ND-2.01	0.31	0.39	ND-2.01	0.44	0.53	ND-1.96	0.33	0.36
HCO_3^{-}	mgL^{-1}	55-210	141.92	46.52	ND-400.00	194.20	99.69	55-400	167	91.2	5-400	188	87.6
F^{-}	mgL^{-1}	ND-0.40	0.11	0.13	ND-14.40	0.43	2.19	ND-14.4	0.50	2.35	ND-0.45	0.085	0.14
As	μgL^{-1}	0.45-8.50	2.32	1.97	0.08-22.10	3.84	4.26	0.18-22.1	2.6	3.85	0.78-17.3	4.13	3.59
Fe	mgL^{-1}	0.02-4.00	1.16	1.44	0.01-5.08	1.01	1.25	0.01-2.89	0.44	0.7	0.02-8.08	1.75	1.47

Total dissolved solids (TDS) are observed to be higher in the north bank compared to the south bank. Local influences on the hydrogeochemistry could account for such variation, while observation of the seasonal trend suggests the elevation of weathering and dissolution processes in the post-monsoon season leading to higher TDS in that season. pH of groundwater in both the north and the south banks were found to be acidic to alkaline. The groundwater of the south bank is slightly more alkaline than the north bank. The pH level in the post-monsoon season appear to be higher than the pre-monsoon season which could be due to dissolution of more carbonate leading to an increase in HCO_3^-. The prevalence of both reducing and oxidizing conditions spatially and seasonally indicate the presence of a mixed aquifer system. However on an average, reducing condition was found to be more dominant than oxidizing condition. Electrical conductivity is higher in the groundwater of the north bank compared to the south bank; this could be due to higher rates of weathering in the former compared to the latter. It appears that the contribution of weathering and dissolution processes are significant in the post-monsoon as much higher EC was recorded in the post-monsoon compared to the pre-monsoon season. The cations Na^+ and K^+ are higher in the groundwater of the north bank compared to that of the south bank which indicates the possibility of more silicate weathering in the north bank compared to the south bank. Silicate weathering seems to be enhanced in the post-monsoon season due to recharge. Calcium and Mg^{2+} have almost similar distribution in both the banks (Table 4.1). Average values of Ca^{2+} and Mg^{2+} in the post-monsoon indicate the elevation in carbonate weathering incidences owing to precipitation. It appears that the level of Cl^- is much higher in the north bank compared to the south bank (Table 4.1). A single incidence of very high Cl^- was found in the north bank owing to the use of bleaching powder [$Ca(ClO)_2$] which could be the possible reason for the above observation. The Cl^- level appears to increase in the post-monsoon which could be due to mobilization of anthropogenic sources during the recharge process. Sulphate and PO_4^{3-} have very low levels and have similar average distributions in both the north and south banks (Table 4.1). The same can be observed for the pre and post-monsoon seasons as well. Nitrate levels are also very low in our study area and the average values are similar bank wise and seasonally. Higher alkalinity in the south bank could be due to greater dominance of carbonate weathering in the south bank compared to the north bank. Carbonate weathering also appears to be

more dominant in the post-monsoon due to recharge which could be the cause of higher HCO_3^- in that season. The F^- level in the BFP was found to be very low. The very high value of F^- (14.4 mgL^{-1}) detected in the south bank was from the Karbi Anglong district which falls outside the BFP region and subsequently was not used during discussion. Seasonal variation also suggests that the overall F^- is quite low. A distinct observation could be made from the As levels of the groundwater in the north and the south banks (Table 4.1). In the north bank the As level of the groundwater was well within the drinking water limit prescribed by WHO [16]. However much higher levels of As which exceeded the WHO limit were detected in the south bank (Table 4.1). Overall the As levels were higher in the post-monsoon season as observed from the higher average values. Iron levels were found to be similar in both banks of the BFP (Table 4.1). However it appears that Fe is mobilized during the post-monsoon season as shown by the higher values in that season.

4.3.1.2. Mineralogy

Mineralogy was obtained by XRD analysis of the grab sediment samples (Table. 4.2, Fig. 4.1, 4.2 and 4.3). Besides these clay minerals, montomorillonite has also been reported in the sediments [37]. Jain et al [37] revealed that in the BFP illite, kaolinite and chlorite percentages are 62.5%, 18.81% and 18.85% respectively.

Table 4.2: Results of XRD analysis showing the mineralogy of the sediments

Serial	Sampling sites	Sediment type	Minerals
BRS-1	Guijan	Sand	Delhayelite, Anorthoclase, Inyoite ,Paragonite & Trollite.
BRS-2	Rohmoria	Loam	Rutile, Anorthoclase, Sanidine.
BRS-3	Dibrugarh	Sand	Rutile, Opal & Silica.
BRS-4	Nimatighat	Clay loam	Rutile, Opal & Quartz
BRS-5	Dhansirimukh	Loamy sand	Rutile, Opal, Quartz & Arsenopyrite
BRS-6	Tezpur	Loam	Rutile & Opal.
BRS-7	Guwahati	Loam	Rutile, Riebeckelite,Walpurgite, Biotite & Vermiculite
BRS-8	Jogighopa	Sand	Labradorite, Trollite

BRS stands for Brahmaputra River Sediment

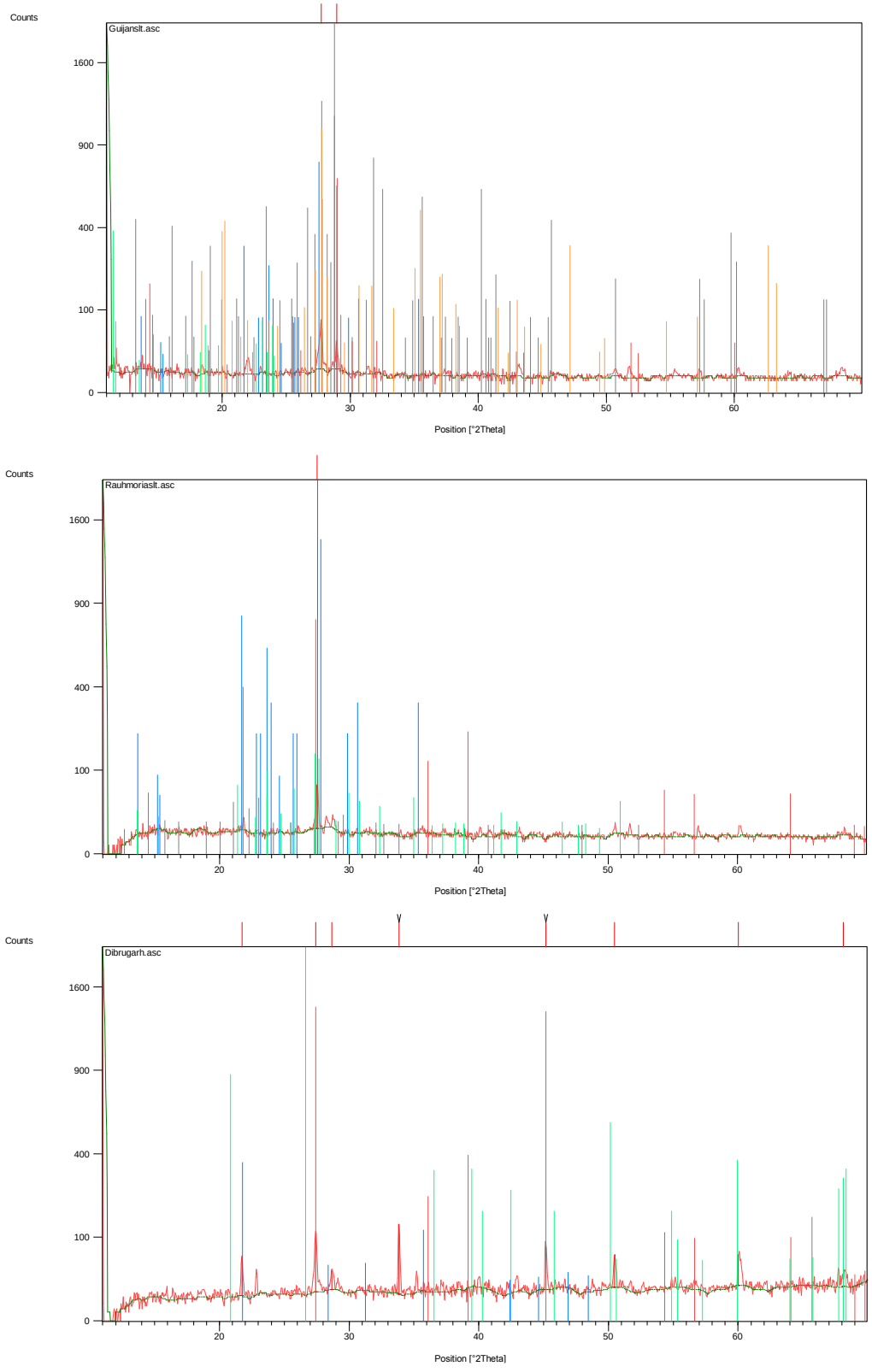

Figure 4.1: XRD diffraction patterns for BRS-1, 2 and 3

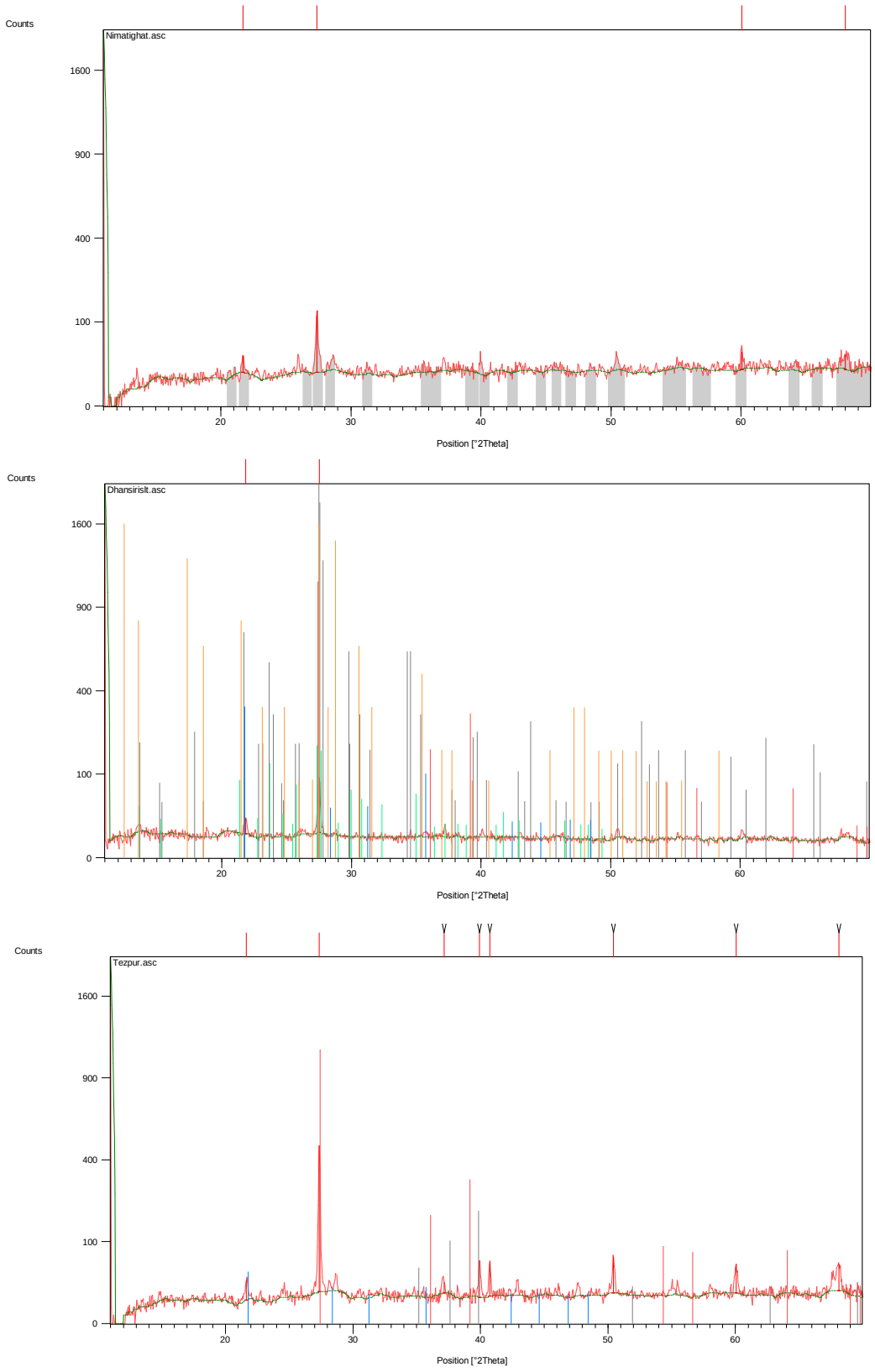

Figure 4.2: XRD diffraction patterns for BRS-4, 5 and 6

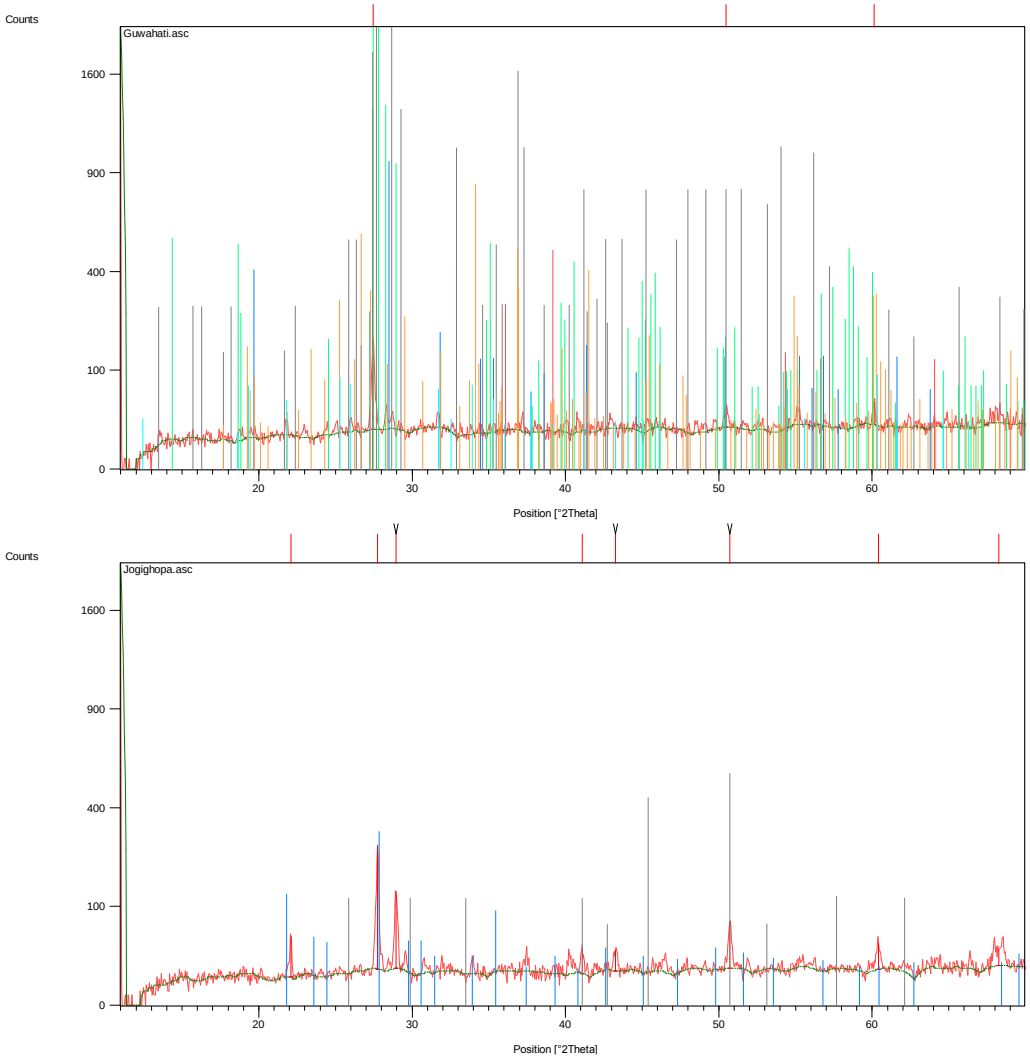

Figure 4.3: XRD diffraction patterns for BRS-7 and 8

A powder X ray diffraction technique was applied to identify the non-clay minerals in the sediment samples collected throughout the whole stream. Rutile was found in most of the sediments. An interesting finding from XRD study was the presence of the mineral Arsenopyrite (FeAsS) in the grab sediments samples collected from the BFP (Table. 4.2). Arsenpyrite was detected in one sample marked BRS-5, while walpurgite [$Bi_4(UO_2)(AsO_4)_2O_4$•$2(H_2O)$] was detected in sample BRS-7 (Table. 4.2). The probable reason for detection of As minerals in only two of the sediment samples could be the low number of sediment sampling spread over a large area i.e., BFP.

4.3.1.3. Hydrochemical facies

The hydrochemistry of the groundwater of an area evolves due to the interaction between various minerals and ions of the aquifers [38, 39, 40, 41]. The raw data obtained from analysis of various parameters like the major ions, pH and TDS, can be used to generate the Piper diagram [41, 42]**.** This diagram can be used to classify water into facies or types which are indicative of the hydrochemical processes occurring in the study area. This diagram can also be used to determine recharge and discharge in a study area. Subsequently, Piper diagrams were prepared to observe both spatial as well as seasonal variations. In our study we found that in the north bank HCO_3^- was shared equally by the cations Ca^{2+}, Mg^{2+}, Na^+ and K^+, while other anionic phases had minor occurrence (Fig. 4.4a). In the south bank also, Ca^{2+}-Mg^{2+}-HCO_3^- and Na^++K^+-HCO_3^- were the two major water types (Fig. 4.4b), the former had higher occurrence than the latter. It can also be observed that samples with As > 10 μgL^{-1} occurred in the HCO_3^- water type. Moreover, it can be observed that local hydrochemical affects are more prominent in the north bank compared to the south bank as three distinct regions can be observed in the diamond of the north bank (Fig. 4.4a). HCO_3^- type water with mixed contribution from the cations Na^+, K^+, Ca^{2+} and Mg^{2+} appear to be common in both pre as well as post-monsoon seasons (4.3c and d). However closer observation reveals that HCO_3^- type water is more common in the post-monsoon. Overall high As was found to be associated with HCO_3^- type water in both pre and post-monsoon seasons, indicating the influence of alkaline environment in enhancing groundwater As.

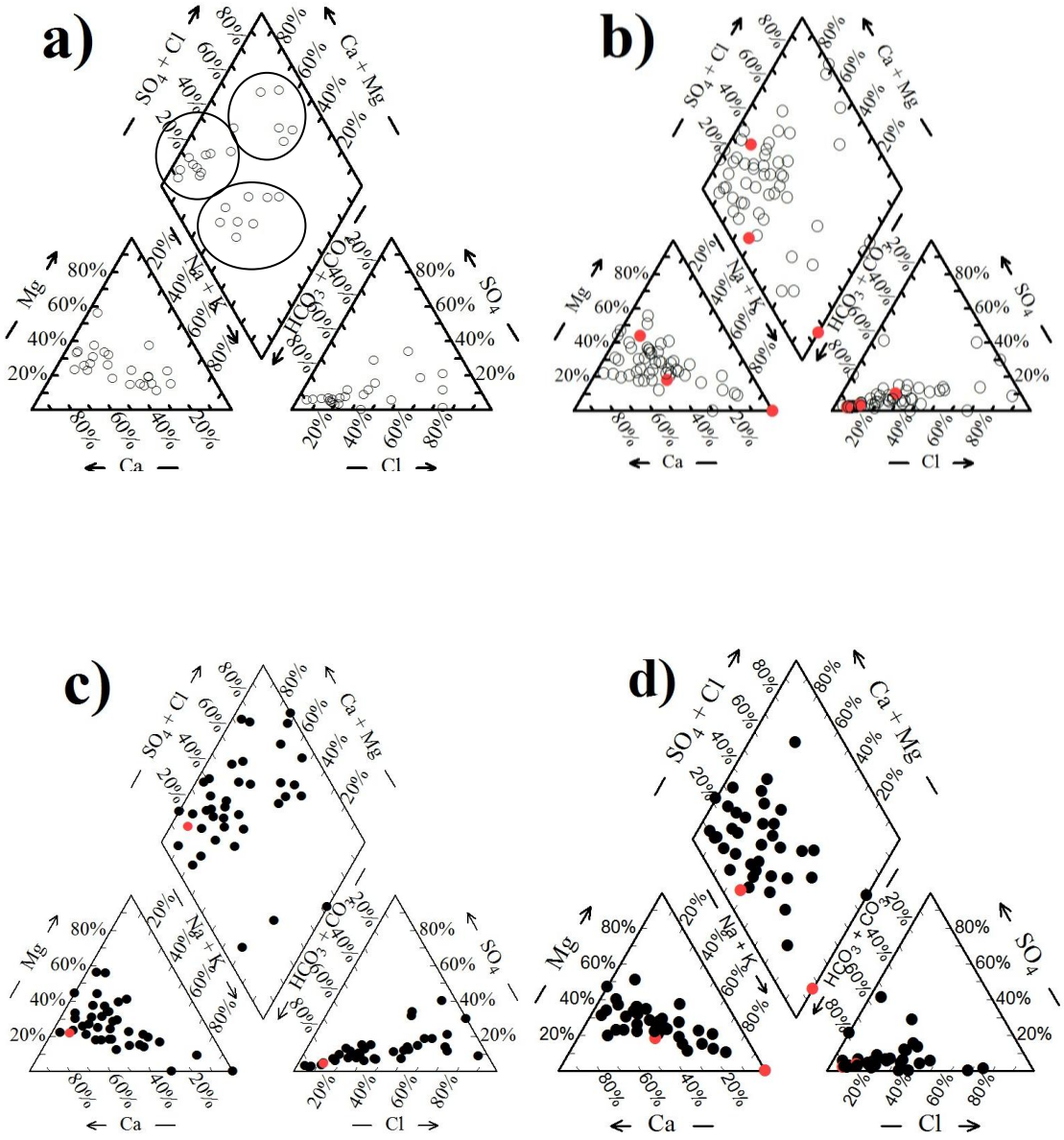

Figure 4.4: Piper diagram showing the different groundwater types in the (a) north, (b) south banks of the BFP, (c) pre-monsoon and (d) post-monsoon seasons. The red solid circles indicate groundwater samples with As level > 10 µgL^{-1}

4.3.1.4. Hydrogeochemical evaluation

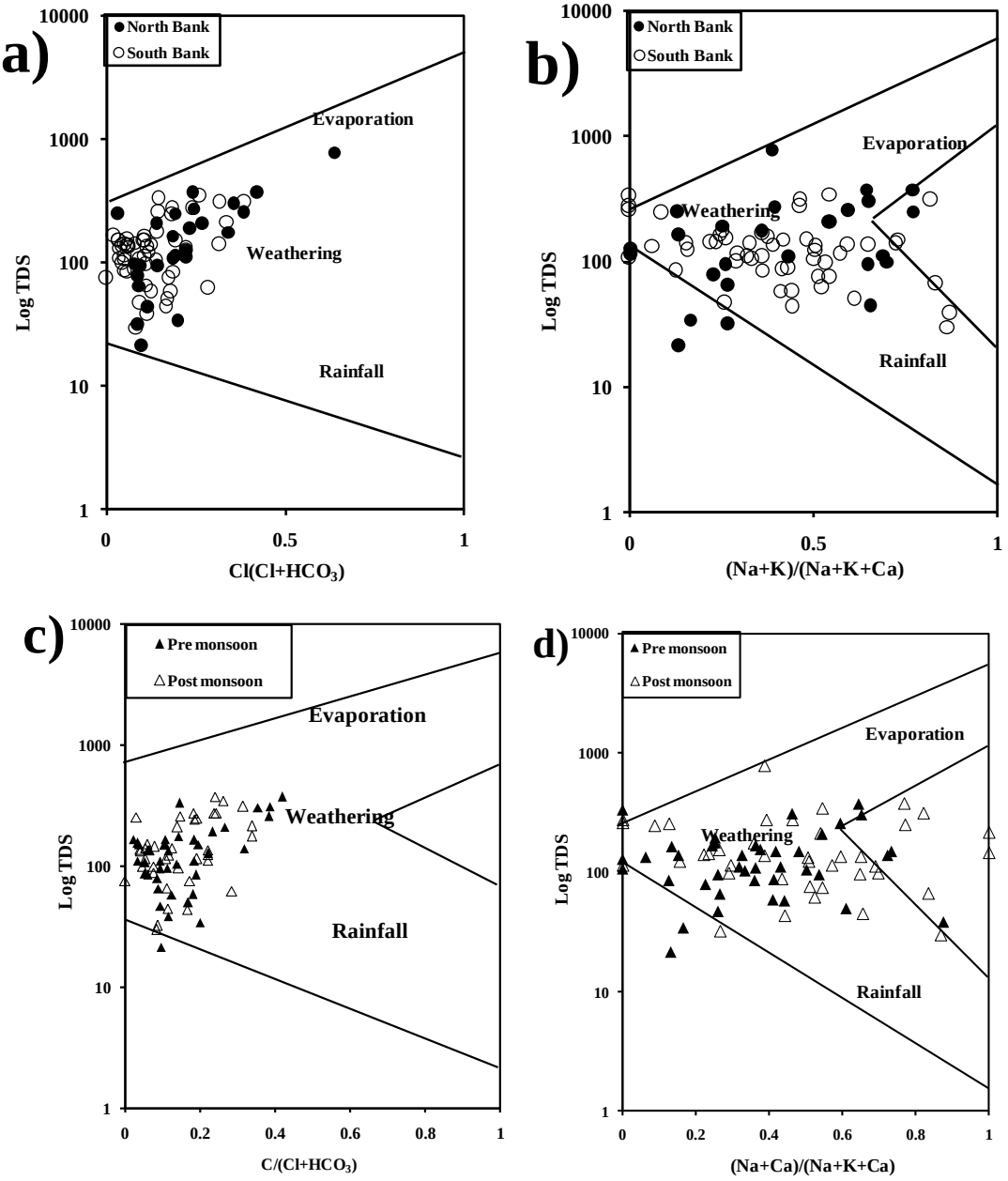

Figure 4.5: Gibbs plots showing that rock-water interaction controls the groundwater chemistry both (a, b) spatially and (c, d) seasonally

The preliminary investigation of the hydrogeochemical processes was done by making the Gibbs plots (Fig. 4.5) [43] in order to identify the nature of processes operating in the aquifers of the study area. Influence of rock dominance, evaporation and

precipitation can be identified using the Gibbs plots, log TDS versus (Na+K)/(Na+K+Ca) ($meqL^{-1}$) and log TDS versus Cl/(Cl+HCO_3) ($meqL^{-1}$). Weathering and dissolution processes appear to be the dominant processes both, spatially and seasonally.

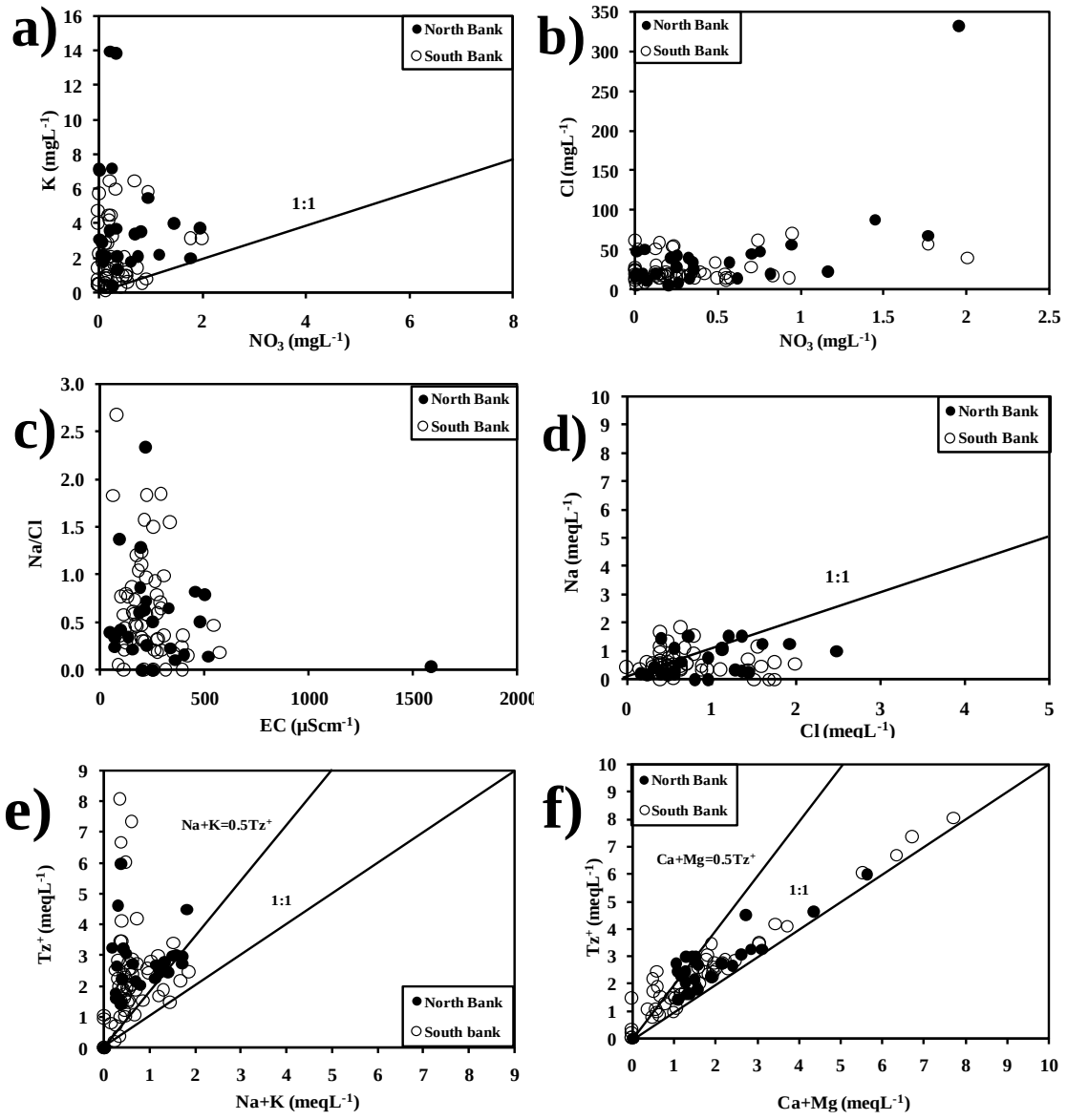

Figure 4.6: Scatter plots for investigating the hydrochemistry of the north and the south banks. (a) NO_3 versus K (b) NO_3 versus Cl (c) EC versus Na/Cl molar ratio, (d) Cl versus Na, (e)Tz^+ versus Na+K and, (f) Tz^+ versus Ca+Mg

The NO_3^- level is a good indicator of drinking water suitability and anthropological interference in groundwater, since the common sources of this contaminant are leachates from landfill sites, agricultural run offs, domestic sewage etc. The NO_3^- level in the groundwater of the BFP was found to be very low. Nitrate could act as one of the donors of oxygen for bacterial degradation of organic matter which could lead to reducing conditions in the aquifers. Although the negative ORPs in majority of the groundwater samples indicate the presence of a reducing condition in both the north and south banks, it is unlikely that NO_3^- is driving the process as the values of NO_3^- detected in our study are quite low (Fig. 4.6a). The same observation can also be made for the distribution of NO_3^- in the pre and post-monsoon season (Fig. 4.7a). Lack of much seasonal variation indicates that anthropogenic influences on the contamination of groundwater by NO_3^- are very meagre. A similar trend was observed in the plot of NO_3^- versus K^+ both spatially (Fig. 4.6a) and seasonally (4.7a). Most of the points were found to lie above the 1:1 line indicating different sources for both, as there is an excess of K^+ compared to NO_3^-. The source of K^+ could be silicate weathering, which is discussed later, while NO_3^- could come from anthropogenic sources. A few of the samples do fall along 1:1 line indicating the presence of anthropogenic fertilizer usage or other similar sources of K^+ and NO_3^-. While the plot of Cl^- versus NO_3^- show that there is a weak relationship between the two (Fig. 4.6b), the relationship is more prominent in the north bank, proving that both Cl^- as well NO_3^- could originate from common anthropogenic sources in some samples. A very high level of Cl^- is observed in a single groundwater sample in the north bank (Fig. 4.6b). Use of potash (KCl) doesn't appear to be the source; locally used bleaching powder [$Ca(ClO)_2$] seeping into groundwater could be the probable reason. Observation of the seasonal variation showed that the relationship between Cl^- and NO_3^- is weak, however the relationship is slightly stronger in the post-monsoon season (Fig. 4.7b), which could be due to mobilization of anthropogenic sources during recharge processes. The plot for Na^+/Cl^- versus EC shows that there is no relationship between Na^+/Cl^- molar ratio and EC both spatially (4.5c) and seasonally (4.6c). Therefore further investigation was carried out by plotting the Na/Cl scatter diagram. The molar ratio of Na^+/Cl^- will be approximately 1 if halite dissolution is the dominant process operating in the system and Na^+ and Cl^- will be equally released due to the process. If the ratio is >1 then silicate weathering is considered to be the

governing process for sodium dissolution [41, 44, 45, 46]. Evaporation is the dominant process if the points shift down below 1 leading to an abundance of Cl^-. In our study the two dominant processes appear to be evaporation and silicate weathering, both silicate weathering and evaporation are equally dominant in the south bank while evaporation is more dominant in the north bank (Fig. 4.6d). It can be observed that silicate weathering is slightly more pronounced or dominant in the post-monsoon season (4.6d). Silicate weathering is considered to be one of the most important geochemical processes operating in groundwater; the process is especially significant in hard rock aquifers [41, 47, 48, 49]. The contribution to silicate weathering can be analysed by studying the plots of Na^++K^+ and Ca^{2+}+ Mg^{2+} versus total cations (Tz^+). In the plot of Na^++K^+ versus Tz^+, most of the samples in both the north and the south banks show silicate weathering as the groundwater samples are situated along the silicate weathering line ($Na+K=0.5Tz^+$) (Fig. 4.6e) [44, 49]. The same can also be observed for the pre and post-monsoon seasons (Fig. 4.7e). The probable silicate species involved in releasing Na^+ and K^+ into the groundwater could be albite (soda feldspar) and, orthoclase and microline (potash feldspar). Feldspar has been suggested over quartz because the latter has been found to be more resistant to weathering and changes in silicate rocks [49]. It can be observed that contributions due to non-silicate minerals like mirabilite ($Na_2SO_5 \cdot 10H_2O$) or anthropogenic sources cannot be ruled out [50] especially in the south bank and the post-monsoon season, as some points are observed to fall along the 1:1 line (Fig. 4.6e and 4.7e). This could be due to anthropogenic activities like higher usage of fertilizers in the south bank compared to the north bank. The same observation in the post-monsoon season could be observed due to mobilization of anthropogenic inputs induced by precipitation. The plot of Ca^{2+}+Mg^{2+} versus Tz^+ shows that most of the samples lie between the 1:1 and the $Ca+Mg=0.5Tz^+$ lines in both banks (Fig. 4.6f) as well as seasons (Fig. 4.7f) indicating the role of silicate weathering in releasing Ca^{2+} and Mg^{2+} in the groundwater [49].

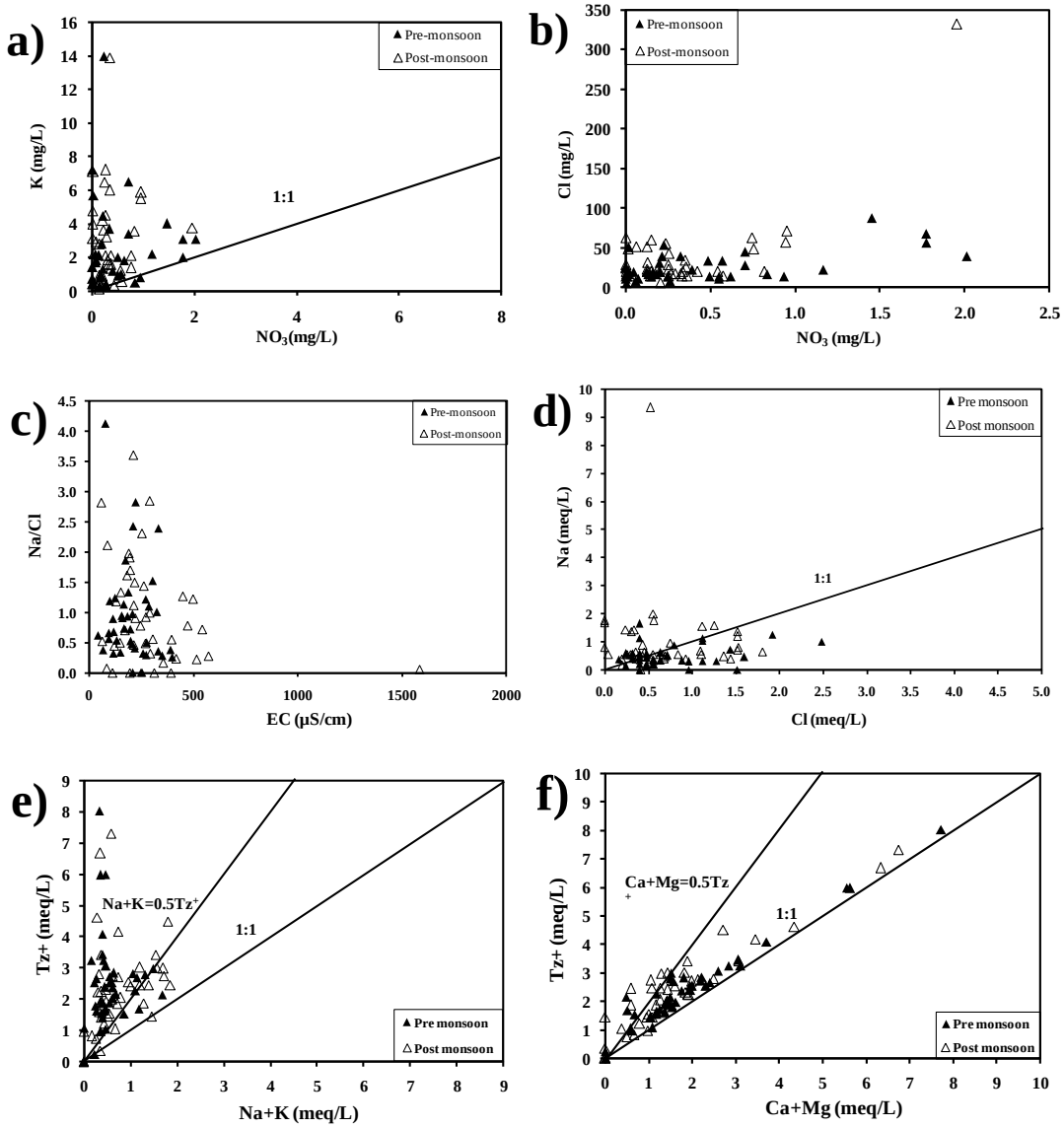

Figure 4.7: Scatter plots for investigating the hydrochemistry of the pre and post-monsoon. (a) NO_3 versus K, (b) NO_3 versus Cl, (c) EC versus Na/Cl molar ratio, (d) Cl versus Na, (e)Tz^+ versus Na+K and, (f) Tz^+ versus Ca+Mg

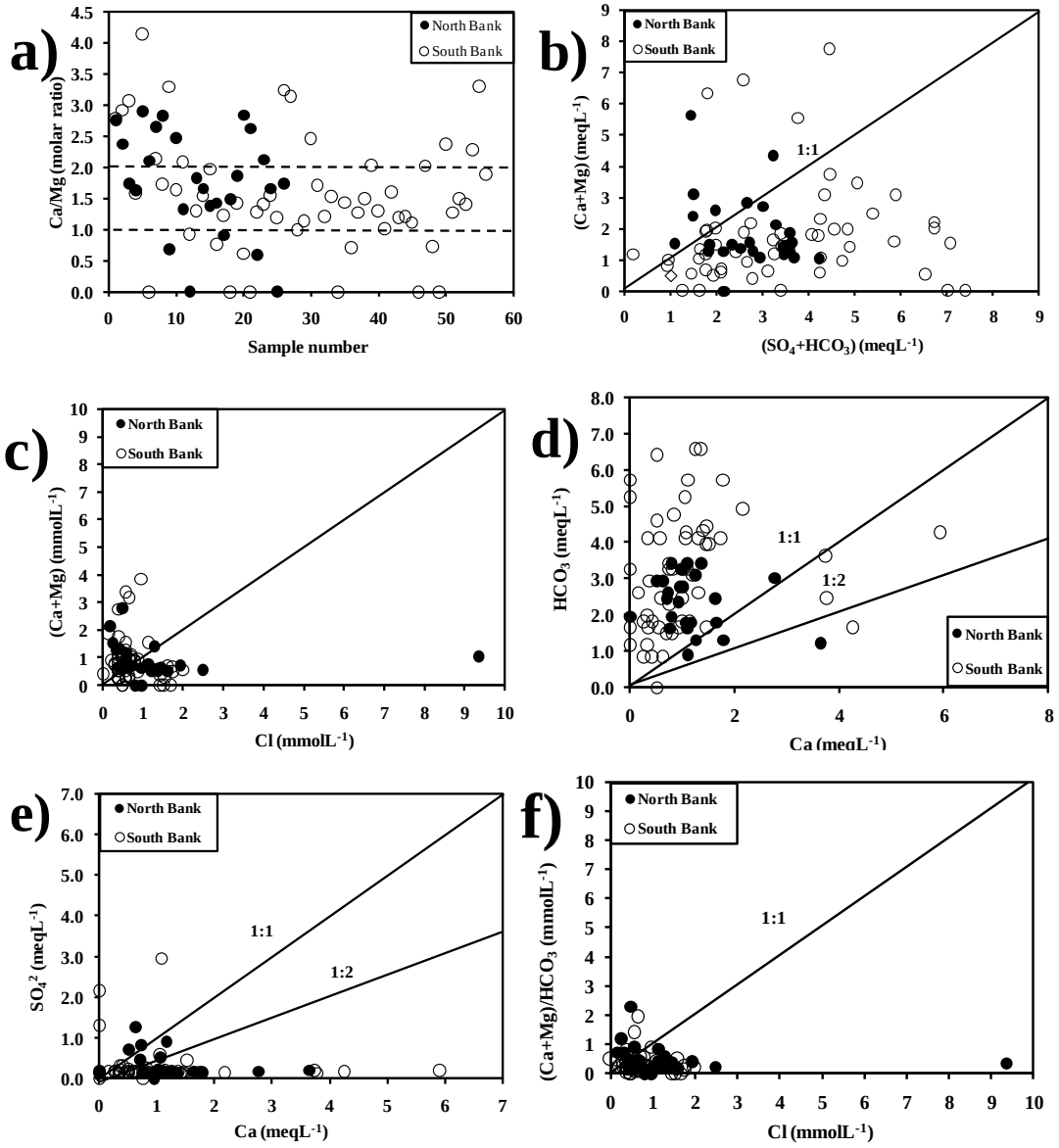

Figure 4.8: Scatter plots for investigating the spatial trends of carbonate weathering in the BFP

Ca^{2+}/Mg^{2+} molar ratio is reported to be an indicator of the presence of calcite and dolomite dissolution in the study area [41]. If the ratio of Ca^{2+}/Mg^{2+} is close to 1 then it is inferred as an indicator of dolomite dissolution, a ratio >1 (1 to 2) is reported to represent higher calcite dissolution [51]. Silicate weathering and dissolution is the chief process if Ca^{2+}/Mg^{2+} ratio is >2. It can be observed that both silicate and carbonate weathering are dominant processes in the two banks of the river Brahmaputra (Fig 4.8a). In the north bank, both processes appear to be equally dominant. Overall

however, carbonate weathering; especially calcite dissolution appears to be more dominant than silicate weathering. Impact of seasonal variation is clearly visible; it can be observed that calcite weathering is more dominant in the post-monsoon season (Fig. 4.9a). This could be due to higher incidences of weathering and dissolution brought about by precipitation. The plot of (Ca^{2+}+Mg^{2+}) versus (SO_4^{2-}+HCO_3^-) (Fig. 4.8b) reveal that ion exchange processes are dominant in both the north and south banks, as most points lie below the 1:1 equiline. Points lying close to or on the 1:1 line represent dolomite, calcite and gypsum dissolution [41, 52- 54]. Reverse ion exchange leads to enrichment of Ca^{2+} and Mg^{2+} and depletion of Na^+ and K^+, the process is more common in the north bank compared to the south bank. The process of ion exchange is also dominant in both the pre and the post-monsoon seasons, while reverse ion exchange is found to be a minor occurrence (Fig. 4.9b). Closer observation reveals that reverse ion exchange is slightly more common in the pre-monsoon compared to the post-monsoon (Fig. 4.9b). This could be due to the fact that in post-monsoon season precipitation induced carbonate weathering becomes more common and reverse ion is diminished further. The plot of Ca^{2+}+Mg^{2+} and Cl^- ($mmolL^{-1}$) (Fig. 4.8c and 4.9c) do not show any significant trend both spatially and seasonally. The source of Ca^{2+} in the groundwater has been studied further using the plots of Ca^{2+} versus HCO_3^-. Carbonic acid and sulphuric acid are reported to be two of the major agents of weathering in groundwater, if the ratio of Ca^{2+} to HCO_3^- is 1:2 then the source of Ca^{2+} is calcite dissolution [41, 55]. However a ratio of 1:4 is reported to indicate dolomite dissolution. Most of the samples lie above the 1:1 line near the region where Ca^{2+}:HCO_3^- ratio is close to 1:2 (Fig. 4.8d) [49]. The same can be observed from seasonal variation as well (4.8d), indicating the dominance of carbonate weathering both spatially and seasonally. This is confirmed by the plot of Ca^{2+} versus SO_4^{2-}, most of the samples in both the north and the south banks (Fig. 4.8e) and pre and post-monsoon seasons (Fig. 4.9e) lie below the 1:2 line. Thus Ca^{2+} increases without an increase in SO_4^{2-} which indicates that gypsum is not the likely source of Ca^{2+} but calcite weathering is a probable source [49, 56].

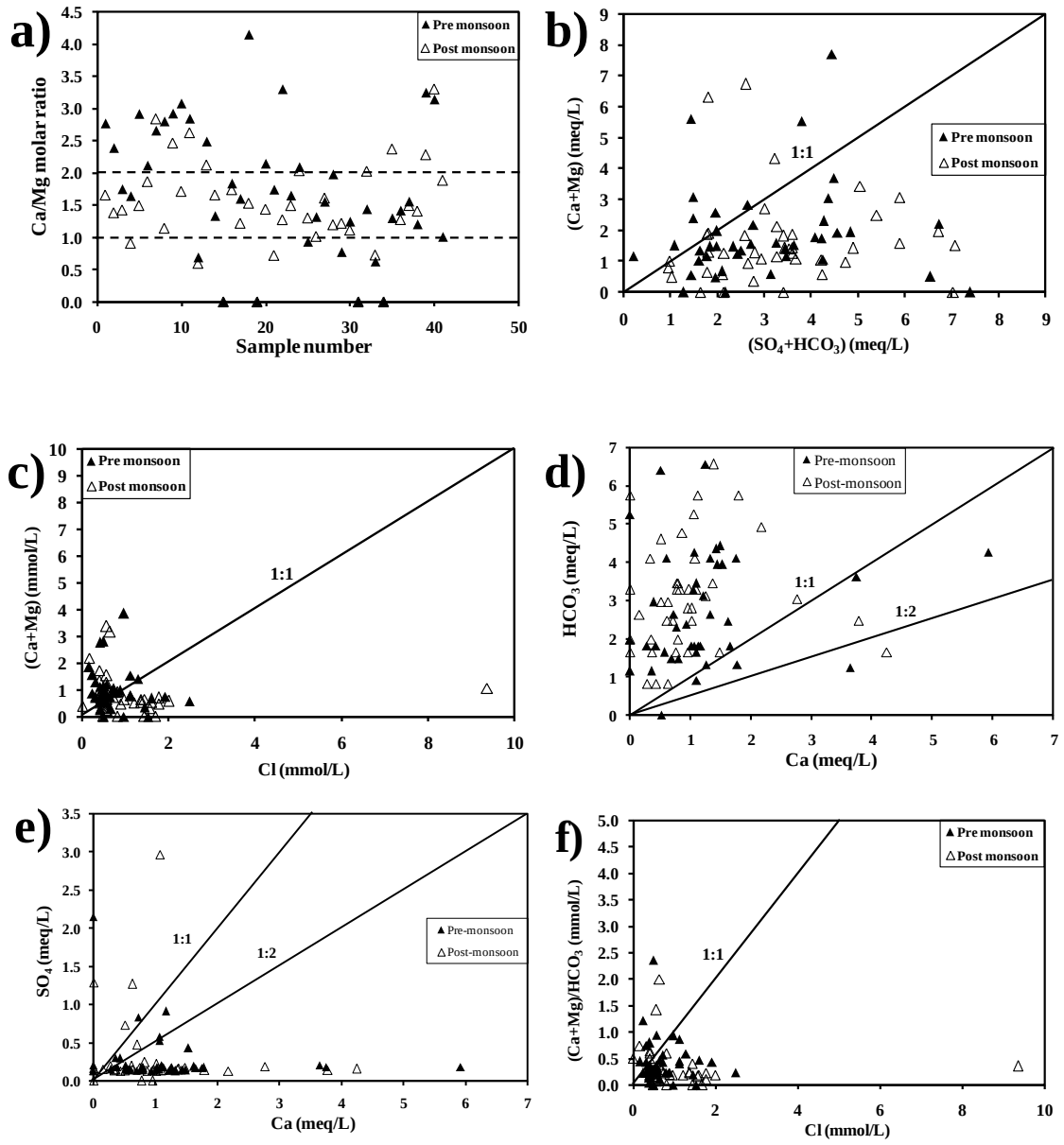

Figure 4.9: Scatter plots for investigating the seasonal trends of carbonate weathering in the BFP

The plot of $(Ca^{2+}+Mg^{2+})/HCO_3^-$ and Cl^- ($mmolL^{-1}$) shows that $(Ca^{2+}+Mg^{2+})/HCO_3^-$ ratio does not increase with the increase in salinity [54]. Thus Ca^{2+} and Mg^{2+} is added at a much slower rate than HCO_3^- in both the banks (Fig. 4.8f) as well as throughout the year (Fig. 4.9f). Thus calcite weathering is the source of Ca^{2+} in our study area, if the opposite had been observed, then silicate weathering could have been more prominent.

4.3.1.5. Distribution of arsenic and fluoride

Spatial distribution of arsenic: Most of the groundwater samples in this study had As values within the limit permitted by WHO [16] for drinking water. The permissible limit was exceeded in only three of the groundwater samples from the south bank. The highest As level of 22.1 μgL^{-1} was detected in Naltali in Nagaon district of Assam, India close to the Brahmaputra River. The other two groundwater samples which had high As were from the Jorhat district of Assam, India. The observed concentrations of As in those two samples were 17.3 and 16.74 μgL^{-1}. We found in our study that As level decreases with depth in both the north and the south banks of the BFP, the relation is more prominent in the south bank than in the north bank (Fig.4.10a). It was reported by [57] that with increasing depth the condition becomes highly reductive, ultimately to the point that the free As starts to precipitate out by forming sulphides, this could explain the reduction in As levels with depth. A reducing condition was observed in a number of groundwater samples in both the north and the south banks, and it was found that As level varied inversely with redox conditions, implying that a reducing condition favoured the release of groundwater As (Fig 4.10b). The above observation could mean that reductive hydrolytic processes are found in both the banks and could act as the pathway of As mobilization. In the next plot the relationship between As and Fe (Fig.4.10c) was observed and it was found that As increased linearly with an increase in Fe levels in the groundwater. The presence of an inverse relation with ORP and a positive relation with Fe indicates the presence of reductive dissolution of Fe (hydr)oxides in the BFP region. The scatter plot of As versus pH shows that groundwater As is distributed over a pH range of about 5 to 10 (Fig. 4.10d) and a gradual rise is observed in the As level with the increase in pH values.

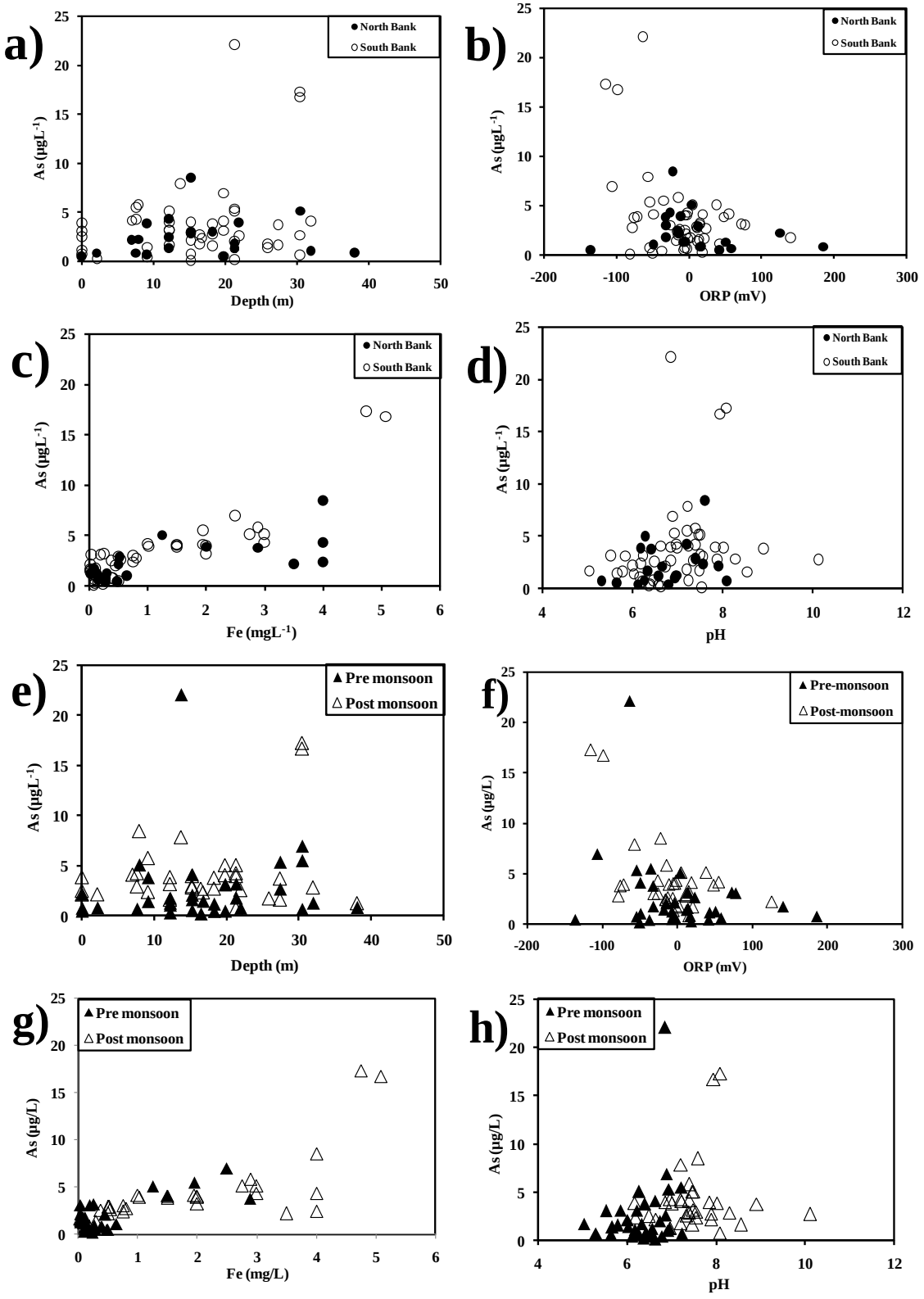

Figure 4.10: Comparison of As behaviour with other parameters spatially and seasonally

Seasonal distribution of arsenic: The highest level of groundwater As was detected in the Naltali area of Nagaon district (22.1 μgL^{-1}) during the pre-monsoon season. In the post-monsoon two groundwater samples were found to have As above 10 μgL^{-1} in the Jorhat district, the detected As levels were 17.3 and 16.74 μgL^{-1}. A distinguishing trend between As and depth was not observed in the BFP area. In the pre-monsoon season As level >10 μgL^{-1} was found in a single tube well with a shallow depth of 13.72 m, but in the post-monsoon season it was observed that higher levels of As was found in two tube wells with depth of approximately 30.5 m each. For the samples with As levels within the permissible limit, it was observed that As level decreased with depth in the post-monsoon season, while suitable relation is missing in the pre-monsoon (Fig. 4.10e). The reducing condition which is prevalent in the BFP is evident from the largely negative ORPs of the region (Table. 4.1). It can be observed that a negative correlation is observed between ORP and the groundwater As level in both pre and post-monsoon seasons (Fig. 4.10f). This is indicative of groundwater As enhancement by the prevailing reducing conditions. In order to observe the presence or the absence of reductive hydrolysis of Fe (hydr)oxides the relationship between As and Fe was observed (Fig. 4.10g). It was seen that As showed good correlation with Fe level in the groundwater samples, with regression coefficients of R^2=0.57 and R^2=0.52 respectively for pre and post-monsoon seasons. Correlation analysis has also been utilized later in the chapter to analyse the relationship of As and Fe. It was found that the two shared very good correlation in both pre and post-monsoon seasons (Table. 4.5 and 4.6). This confirms that reductive hydrolysis of Fe (hydr)oxides is the principal mode of As mobilization in the BFP throughout the year. A strong relation is not observed between As and pH, however it appears that the process of As mobilization is influenced by increase in pH levels (Fig. 4.10h). Increase in pH level has been linked to desorption of adsorbed As oxyanions from positive surfaces like Fe (hydr)oxides [57]. At acidic pH Fe (hydr)oxides have been found to have a net positive charge on their surfaces enabling them to adsorb negatively charged anions like As oxyanions. With an elevation in pH the charge equilibrium shifts towards negative leading to desorption of adsorbed anions. The highest desorption has been found to occur at pH > 8.3 when the surface charge is close to zero due to achievement of the point of zero charge (PZC) [6, 57].

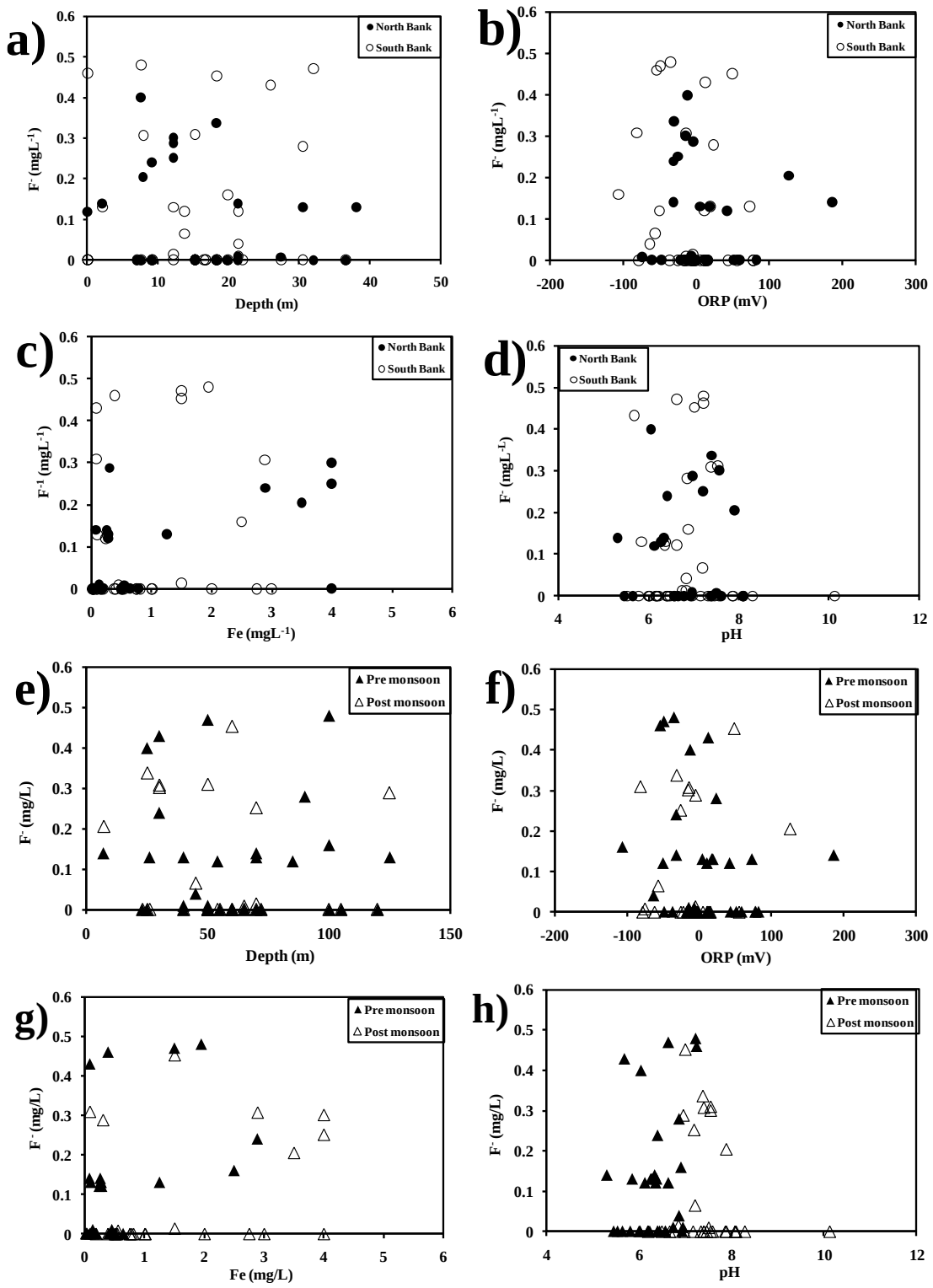

Figure 4.11: Comparison of F^- behaviour with other parameters spatially and seasonally

Spatial distribution of fluoride: The F^- values in our studies were found out to be very low; all the values were below the permissible limit for F^- in drinking water given by WHO [16]. The probable reason could be that the fluvial environment is not suitable or doesn't promote the enrichment of F^- which we had already discussed in the literature review chapter. Even if F^- does occur in floodplain regions, there is a high probability of its occurrence in areas which are cut off from frequent groundwater recharge sources like rivers. In our study we could not find any relationship between F^- and depth (Fig. 4.11a). When F^- and redox potential was plotted, although we failed to observe a proper relation between the two (Fig.4.11b), yet we found a poor negative relation between the two. The reason for the weak relation could be that many of the groundwater samples in ours study had F^- level below the detection limit of the instrument and the F^- values were registered as zero. No trend was observed between Fe and F^- in either banks of the BFP (Fig. 4.11c). Lastly in the plot of pH versus F^- also, we couldn't find any observable trend between the two because of the extremely low values of F^- in our study (Fig. 4.11d).

Temporal variation of fluoride: Seasonal variation was not found to have any profound impact on the F^- mobilization process in the BFP. Due to the extremely low levels of F^- in BFP, the scatter plots yielded inconclusive results. Fluoride did not show variation with depth in both the pre as well as the post-monsoon seasons (Fig. 4.11e). Fluoride appears to be prevalent in both reducing as well as oxidizing conditions and a slight negative correlation is observed between groundwater F^- levels and ORP (Fig. 4.11f). The groundwater Fe level also does not appear to have any influence on F^- enhancement as no relationship is observed between the two (Fig. 4.11g). It has been reported that F^- level is positively influenced by elevation in pH and an alkaline condition [34, 35]. However in our study we failed to observe any defining correlation between the two paramters (Fig. 4.11h).

4.3.1.6. Statistical analysis

4.3.1.6.1. Correlation analysis

Spatial variation: Correlation analysis, a bivariate statistical tool, was used to observe the relation among the 16 variables in this study. Subsequently the correlation matrix was prepared for TDS, pH, ORP, EC, Na^+, K^+, Ca^{2+}, Mg^{2+}, Cl^-, SO_4^{2-}, PO_4^{3-}, NO_3^-, HCO_3^-, F^-, As and Fe using the software package SPSS 20 (Table. 4.3 and 4.4). Evaporation and salt dissolution appears to be important processes in both the north and the south banks as Cl^- share positive correlation with EC and TDS on both sides of the river Brahmaputra (Table 4.3 and 4.4). In the north bank, anthropogenic sources like improper sewage disposal could account for the positive correlation between Cl^- and NO_3^- (Table 4.3). A similar correlation is missing in the south bank which could be due to better sanitary facilities or drainage conditions which prevents the leaching of Cl^- and NO_3^- to groundwater. Carbonate weathering (dolomite) also appears to be an important hydrochemical process in BFP. It can be observed that in both banks, a good positive correlation is observed between Ca^{2+} and Mg^{2+}. The higher correlation of Ca^{2+} and Mg^{2+} in south bank also implies higher incidences or rates of carbonate weathering in the south bank. A positive correlation is observed between F^- and SO_4^{2-} in the south bank. The probable cause could be that both the anionic species are adsorbed and desorbed on similar positively charged surfaces like oxides and hydroxides of metals. In the north bank F^- and Fe share a positive correlation which indicates that positively charged Fe (hydr)oxides may act as a source of F^-. The most important observation appears to be the positive correlation between As and Fe in both the north and the south banks of the BFP. This indicates the possibility of reductive hydrolysis of Fe (hydr)oxides as the pathway of As release in the groundwater on both sides of the BFP.

Table 4.3: Correlation matrix for the groundwater parameters of the north bank

	TDS	pH	ORP	EC	Na^+	K^+	Ca^{2+}	Mg^{2+}	Cl^-	SO_4^{2-}	PO_4^{3-}	NO_3^-	HCO_3^-	F^-	As
pH	.023														
ORP	-0.16	-0.40													
EC	**0.86**	0.37	-0.23												
Na^+	0.13	0.23	0.23	-0.10											
K^+	0.21	0.21	-0.10	0.07	0.49										
Ca^{2+}	-0.09	0.02	-0.16	0.05	-0.49	0.04									
Mg^{2+}	-0.08	0.11	-0.06	0.08	-0.35	0.19	**0.69**								
Cl^-	**0.86**	0.17	-0.05	**0.87**	0.05	-0.01	-0.14	-0.10							
SO_4	0.28	-0.15	0.06	0.01	0.41	0.10	-0.30	-0.26	0.07						
PO_4	-0.07	-0.20	-0.01	-0.07	-0.24	0.06	**0.65**	0.43	-0.14	0.12					
NO_3^-	**0.63**	0.02	0.27	0.45	0.19	-0.17	-0.30	-0.21	**0.67**	0.24	-0.23				
HCO_3^-	0.15	**0.53**	-0.32	0.26	0.19	-0.12	-0.27	-0.19	0.22	0.08	-0.38	0.09			
F^-	0.43	-0.05	-0.03	0.28	0.18	0.29	-0.27	-0.32	0.37	-0.13	-0.16	0.13	-0.15		
As	0.04	0.27	-0.19	0.22	-0.09	-0.27	-0.13	-0.05	0.02	-0.30	-0.20	-0.21	0.33	0.09	
Fe	0.33	0.39	-0.08	**0.52**	-0.13	-0.17	-0.11	-0.11	0.39	-0.33	-0.17	0.04	0.10	**0.53**	**0.70**

Table 4.4: Correlation matrix for the groundwater parameters of the south bank

	TDS	pH	ORP	EC	Na^+	K^+	Ca^{2+}	Mg^{2+}	Cl^-	SO_4^{2-}	PO_4^{3-}	NO_3^-	HCO_3^-	F^-	As
pH	.033														
ORP	-0.08	-0.45													
EC	**0.77**	0.25	0.05												
Na^+	-0.03	0.13	-0.17	0.07											
K^+	0.38	0.10	0.14	0.49	0.11										
Ca^{2+}	0.11	-0.06	-0.06	-0.08	-0.23	-0.17									
Mg^{2+}	0.15	0.10	-0.25	-0.12	-0.19	-0.25	**0.77**								
Cl^-	**0.77**	0.25	0.05	**0.90**	0.07	0.49	-0.08	-0.12							
SO_4	0.28	0.12	-0.10	0.23	-0.12	-0.08	-0.02	-0.06	0.23						
PO_4	-0.07	-0.02	-0.03	-0.25	0.14	0.18	-0.08	0.04	-0.25	-0.07					
NO_3^-	0.34	-0.16	0.03	0.29	-0.10	0.14	0.06	0.11	0.29	-0.04	-0.10				
HCO_3^-	0.22	0.39	-0.30	0.00	0.13	0.12	0.20	0.22	0	0.22	0.21	0.07			
F^-	0.44	0.02	-0.19	0.30	-0.11	-0.16	-0.13	0.09	0.30	**0.55**	0.02	-0.01	0.23		
As	0.15	0.24	-0.43	-0.06	-0.03	0.20	0.02	-0.07	-0.06	0.04	-0.02	0.08	0.28	0.09	
Fe	0.20	0.46	-0.43	0	0.23	0.17	0.01	0.11	0	0.19	0.02	0.13	0.38	0.22	**0.89**

Table 4.5: Correlation matrix for pre-monsoon season

	TDS	pH	ORP	EC	Na^+	K^+	Ca^{2+}	Mg^{2+}	Cl^-	SO_4^{2-}	PO_4^{3-}	NO_3^-	HCO_3^-	F^-	As
pH	0.17														
ORP	-0.11	**-0.78**													
EC	**0.57**	0.39	-0.27												
Na^+	0.38	0.05	0.05	-0.03											
K^+	**0.64**	-0.06	-0.02	**0.52**	0.29										
Ca^{2+}	0.02	0.14	-0.09	0.06	-0.31	0.02									
Mg^{2+}	0.00	0.34	-0.28	0.26	-0.41	-0.10	**0.66**								
Cl^-	**0.74**	-0.06	0.10	0.25	0.37	0.41	-0.03	-0.16							
SO_4	**0.54**	0.18	-0.08	0.14	0.34	0.23	-0.08	-0.09	**0.54**						
PO_4	0.09	0.30	-0.29	0.25	-0.07	0.10	0.18	0.39	-0.20	0.04					
NO_3^-	0.42	-0.08	0.13	0.14	0.20	0.06	-0.07	-0.04	**0.59**	0.12	-0.27				
HCO_3^-	0.12	**0.52**	-0.39	0.36	0.04	-0.15	0.19	0.21	-0.08	0.20	0.05	0.02			
F^-	0.44	0.23	-0.20	0.11	0.09	0.14	-0.11	0.17	0.26	**0.86**	0.00	-0.05	0.29		
As	0.14	0.25	-0.26	0.28	-0.17	0.10	0.01	-0.03	-0.05	0.04	-0.06	-0.03	0.39	0.13	
Fe	0.12	0.42	-0.43	0.35	0.06	0.05	0.04	0.29	-0.13	-0.05	0.08	0.11	0.45	0.50	0.75

Table 4.6: Correlation matrix for post-monsoon season

	TDS	pH	ORP	EC	Na^+	K^+	Ca^{2+}	Mg^{2+}	Cl^-	SO_4^{2-}	PO_4^{3-}	NO_3^-	HCO_3^-	F^-	As
pH	0.18														
ORP	-0.06	-0.12													
EC	**0.93**	0.10	-0.09												
Na^+	-0.07	0.06	0.02	-0.13											
K^+	0.14	0.15	0.17	0.11	0.39										
Ca^{2+}	0.08	-0.04	-0.12	0.13	-0.24	-0.15									
Mg^{2+}	0.07	0.05	-0.06	0.12	-0.13	0.00	**0.86**								
Cl^-	**0.86**	0.05	0.00	**0.89**	-0.03	0.09	-0.08	-0.06							
SO_4	0.09	-0.00	-0.02	0.05	-0.02	-0.03	-0.07	-0.12	-0.01						
PO_4	-0.14	-0.07	0.23	-0.10	0.01	0.08	-0.07	-0.07	-0.13	-0.08					
NO_3^-	0.74	0.01	0.13	**0.71**	0.01	0.10	-0.03	0.04	**0.74**	-0.02	-0.05				
HCO_3^-	0.05	0.44	-0.13	0.03	0.12	0.04	0.09	0.09	-0.02	0.18	0.26	0.01			
F^-	0.15	-0.12	0.08	0.13	0.02	0.04	-0.27	-0.26	0.30	-0.13	0.03	0.26	-0.12		
As	-0.06	0.11	-0.49	0.02	0.08	-0.14	0.08	-0.07	-0.14	-0.03	0.06	-0.05	0.22	-0.13	
Fe	0.16	-0.00	-0.12	0.31	0.08	-0.12	0.02	-0.06	0.23	0.00	0.03	0.27	0.15	0.31	**0.73**

Seasonal variation: In the pre-monsoon season, both evaporation and salt dissolution play an important role in controlling the hydrochemistry of the region; this is evident from the positive relation between TDS and Cl^- (Table. 4.5). TDS also show moderate relation with EC, K^+ and SO_4^{2-}. pH and HCO_3^- are interdependent on each other in an aquatic system and here also a positive relation is observed between the two in the pre-monsoon season. pH and ORP are negatively correlated to each other in the pre-monsoon season. While both factors are reportedly important in controlling the As release mechanisms in groundwater [6, 57], yet neither show any significant correlation with As in the pre-monsoon. Both Fe and ORP share a weak negative correlation, which could be due to the prevalence of reductive hydrolytic processes in the pre-monsoon. Silicate weathering could account for the moderate positive correlation between EC and K^+ in the pre-monsoon. Also in the pre-monsoon carbonate weathering, possibly dolomite could be the reason for the positive relation observed between Ca^{2+} and Mg^{2+}. Both SO_4^{2-} and Cl^- could act as anions responsible for permanent hardness in the groundwater. Anthropogenic influences could account for their moderate positive relation. In the pre-monsoon season SO_4^{2-} and F^- exhibit a very strong correlation which could be due to their common origin through desorption from positively charged surfaces like Fe (hydr)oxides, this relation has been further explored using multivariate statistical techniques. Iron and As share a good positive relation in the pre-monsoon season. This indicates that indeed the process of reductive dissolution of Fe (hydr)oxides is pathway for As release in the BFP. In the post-monsoon season, incidences of salt weathering and dissolution are more common than in the pre-monsoon. Therefore TDS and Cl^- share a much stronger correlation in this season. TDS also shares a good relation with EC, while anthropogenic inputs from non-point sources could increase in the post-monsoon season as seen from the positive relation between TDS and NO_3^-, and EC and NO_3^-. A good correlation between Cl^- and NO_3^-, confirms that anthropogenic input is higher in the post-monsoon season. Another probable reason could be washing away and mobilization of residual anthropogenic pollutants from the pre-monsoon season. It can be observed that, the correlation between Ca^{2+} and Mg^{2+} is higher in the post-monsoon than in the pre-monsoon season confirming that dolomite weathering is more common in the post-monsoon season. In the post-monsoon season, the environment in the BFP is mostly reducing in nature, and it is observed that Fe and

ORP share a negative correlation. The relation between As and Fe is positive in the post-monsoon season as well, this shows that reductive dissolution of Fe (hydr)oxides is the chief mode of As release in both the seasons.

4.3.1.6.2. Multivariate statistical analysis

I. Principal components analysis

Table 4.7: PCA of the chemical parameters in the groundwater of the north and the south banks

	North Bank			South Bank		
Parameters	**PC1**	**PC2**	**PC3**	**PC1**	**PC2**	**PC3**
TDS	**0.92**			**0.84**		
pH		**0.82**				**-0.78**
ORP		**-0.69**				
EC	**0.90**			**0.96**		
Na^+			**0.89**			
K^+						
Ca^{2+}	**0.90**				**0.92**	
Mg^{2+}	**0.87**				**0.93**	
Cl^-	**0.91**			**0.96**		
SO_4^{2-}			**0.68**		**0.74**	
PO_4^{3-}	**0.75**					**0.79**
NO_3^-		**0.70**				
HCO_3^-		**0.91**				
F^-		**0.91**			**0.77**	
As			**0.89**	**0.88**		
Fe			**0.85**	**0.82**		
% Variance	**33.55**	**27.19**	**22.98**	**32.9**	**23.73**	**16.83**

Spatial variation: In the north bank, the PCA of the parameters resulted in three PCs with 83.73 % variance. The first component accounts for 33.55 % variance and is represented by TDS, EC, Ca^{2+}, Mg^{2+}, Cl^- and PO_4^{3-} (Table 4.7). This component is represented by hydrochemical processes like carbonate weathering and evaporation. Positive loading due to PO_4^{3-} could be due to dissolution of minerals like apatite [$Ca_5(PO_4)_3(F,Cl,OH)$] or due to the involvement of anthropogenic factors like fertilizer usage. The second component is represented by pH, NO_3^-, HCO_3^-, F^-, and ORP, which has a negative loading, together these accounts for 27.19 % variance. An alkaline

reducing condition is represented by PC2 which favours the release of F^- and reduction of NO_3^-; nitrate may be microbially degraded under the reducing condition. The last PC is represented by As, Fe, Na^+ and SO_4^{2-} with 22.98 %; this PC represents the association of As with the Fe in the north bank. The loading of SO_4^{2-} together with As and Fe could mean that SO_4^{2-} could replace As from adsorption sites on Fe (hydr)oxides. It is unlikely that pyrite, sulphide oxidation could be the probable mechanism of As release as the redox condition is not sufficiently oxidizing in the north bank. In the south bank also we obtained three PCs after performing PCA (Table 4.8). The first PC has a variance of 32.9 % and is represented by TDS, EC, Cl^-, As and Fe; ORP has a very weak negative loading (Table 4.8). This PC represents more than a single hydrochemical process, namely evapotranspiration and reductive hydrolysis of Fe (hydr)oxides. The second PC is represented by Ca^{2+}, Mg^{2+}, SO_4^{2-} and F^- with 23.73 % variance. This PC is represented by weathering and ion exchange processes. The last PC has negative loading from pH and positive loading from PO_4^{3-} and has a variance of 16.83 % variance.

Table 4.8: PCA of the chemical parameters in the groundwater of the pre and post-monsoon seasons

	Pre-monsoon			Post-monsoon		
Parameters	**PC1**	**PC2**	**PC3**	**PC1**	**PC2**	**PC3**
TDS	**0.79**			**0.94**		
pH	**0.77**				**0.74**	
ORP	**-0.72**					**0.70**
EC	**0.65**			**0.94**		
Na^+						**0.86**
K^+	**0.84**					**0.83**
Ca^{2+}		**0.87**		**0.95**		
Mg^{2+}		**0.90**		**0.96**		
Cl^-	**0.60**			**0.95**		
SO_4^{2-}		**0.91**				
PO_4^{3-}			**-0.73**			**0.81**
NO_3^-			**0.75**	**0.85**		
HCO_3^-	**0.77**				**0.82**	
F^-		**0.91**				
As	**0.61**				**0.94**	
Fe	**0.68**				**0.84**	
% Variance	**40.89**	**22.49**	**17.45**	**35.96**	**22.49**	**16.04**

Seasonal variation: By using PCA, three components were identified for the pre as well as post-monsoon season with 80.83% and 74.49 %variance respectively (Table. 4.8). The first PC has 40.89 % variance and is represented by positive loadings from TDS, pH, EC, K^+, Cl^-, HCO_3^-, As and Fe; and negative loadings from ORP. This PC appears to be controlled by reductive hydrolytic processes as observed from the high loadings of As and Fe. The process of reductive hydrolysis is influenced by elevation in pH and alkaline environment (Table 4.8), which results in desorption of more As from Fe (hydr)oxides [6, 57]. Silicate weathering and evaporative processes appear to control the groundwater chemistry to a great extent and can be observed to influence TDS and EC strongly. The second PC has a variance of 22.49 % and high loadings from Ca^{2+}, Mg^{2+}, SO_4^{2-} and F^-. The process of carbonate weathering could be a major influence on this PC resulting in release of Ca^{2+} and Mg^{2+}. Although SO_4^{2-} has a high loading on this component, it is unlikely to represent gypsum dissolution, as graphical inference in the previous section indicates the presence of carbonate weathering rather than gypsum weathering. The high loading of SO_4^{2-} and F^- could represent their co-evolution through desorptive processes or their competitive nature for adsorption on positively charged substrates like (hydr)oxides of metals. The last component with 17.45 % variance is represented by positive loading from NO_3^- and negative loading from PO_4^{3-}; this PC could represent anthropogenic inputs to the groundwater. In the post-monsoon, season the first PC is represented by TDS, EC, Ca^{2+}, Mg^{2+}, Cl^- and NO_3^- and has a variance of 35.96 %. Carbonate weathering appears to be more dominating in the post-monsoon season due to the dissolution effect of precipitation, while mobilization of anthropogenic sources like sewage, could account for the high loadings by NO_3^- and Cl^-. The second PC is represented by pH, HCO_3^-, As and Fe with 22.49 % variance indicating the co-evolution of Fe and As from Fe rich complexes. An alkaline environment appear to be conducive in release of As [6, 57]. The last component is represented by ORP, Na^+, K^+, and PO_4^{3-} with 16.04 % variance.

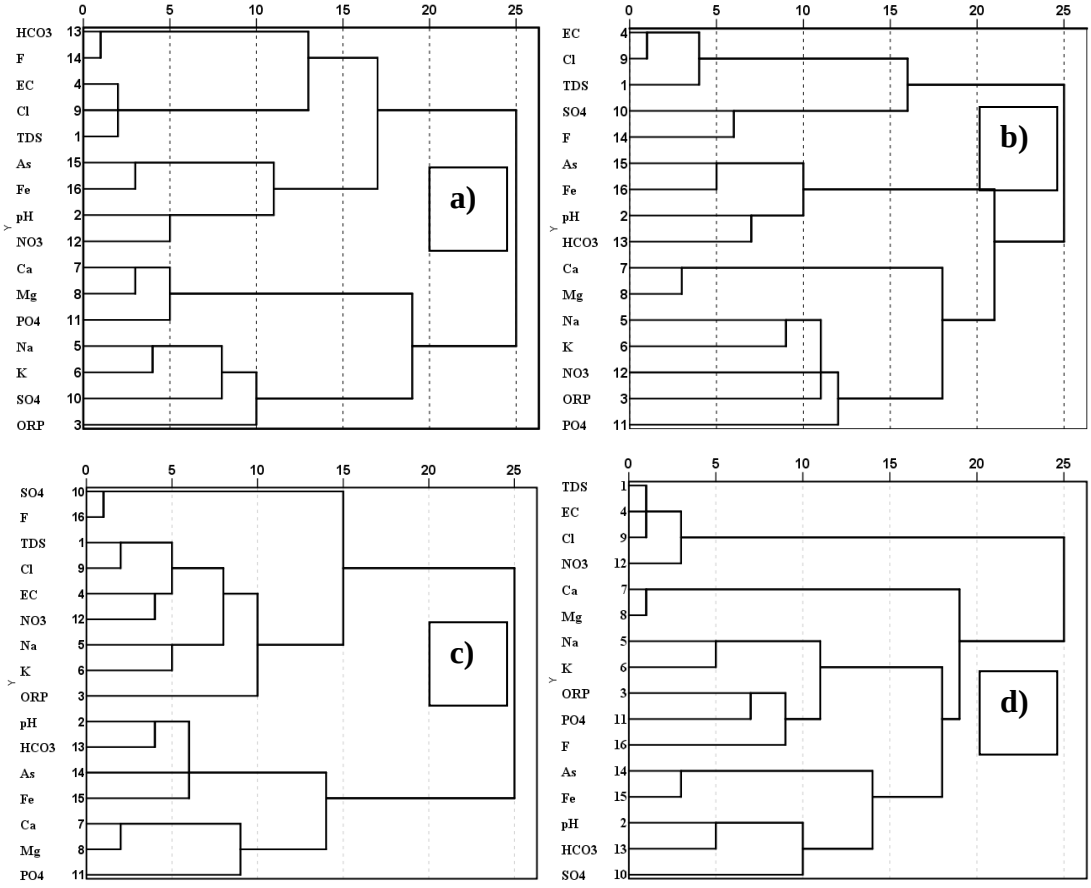

Figure 4.12 Hierarchical cluster analysis (a, b) spatially; and (c, d) seasonally

II. Hierarchical cluster analysis

Spatial variation: It can be observed from the dendrogram generated for the north bank that: As, Fe, pH and NO_3^- are clustered together while F^- is clustered with EC and TDS (Fig. 4.12a). Reductive hydrolysis of Fe (hydr)oxides is the reason behind the clustering of As and Fe together, while elevation in pH could act as one of the triggers for the process. Nitrate could possibly act as a source of oxygen during the reductive hydrolysis process. Fluoride dissolution appears to be affected by an alkaline environment resulting in its clustering with HCO_3^-. Carbonate weathering could be the possible pathway for release of Ca^{2+} and Mg^{2+}, other minerals like apatite [$Ca_{10}(P_4)_6(OH,F,Cl)_2$] could also act as the source of Ca^{2+} in the north bank. Sodium and K^+ are clustered together with SO_4^{2-} indicating that apart from silicate weathering, salts like mirabilite ($Na_2SO_4 \cdot 10H_2O$) and polyhalite [$K_2Ca_2Mg(SO_4)_4 \cdot 2H_2O$] could also be responsible for

releasing Na^+ and K^+ into the groundwater [50]. In the south bank also As and Fe are clustered together indicating that reductive hydrolysis of Fe (hydr)oxides is the process responsible for the mobilization of As (Fig.4.12b). The above process appears to be affected by alkalinity and pH as well. Sulphate and F^- are also clustered together and lie close to the cluster of As, Fe, pH and HCO_3^-. One of the probable reasons could be that Fe (hydr)oxides could act as a probable source of F^- and SO_4^{2-} since both of these are anions and are attracted to positively charged surfaces like metal (hydr)oxides. Sodium, K^+ and NO_3^- are clustered together and could indicate the presence of anthropogenic fertilizer usage in the south bank of the Brahmaputra River.

Seasonal variation: In the pre-monsoon season, (Fig. 4.12c) it can be observed that SO_4^{2-} and F^- are clustered together, this could be due competitive nature of the two anions for adsorption or desorption on/from positively charged surfaces. Silicate weathering and anthropogenic activities could control the cluster represented by TDS Cl^-, EC, NO_3^-, Na^+ and K^+. Clustering of As, Fe, pH and HCO_3^- proves that Fe (hydr)oxides are involved in the process of As mobilization, and the process is influenced by elevation in pH and alkaline conditions. Clustering of Ca^{2+} and Mg^{2+} represents carbonate weathering as the source of the two cations. Phosphate is also represented in this cluster and could represent alternative sources of Ca^{2+} like apatite. In the post-monsoon, (Fig. 4.12d) it is observed that TDS, EC, Cl^- and NO_3^- are clustered together. This represents weathering and dissolution of salts and possibly the mobilization of previously static anthropogenic influxes under the influence of precipitation. Clustering of Ca^{2+} and Mg^{2+} represents the involvement of carbonate weathering in the post-monsoon due to high precipitation rates. Sodium and K^+ represent silicate weathering which also appears to be enhanced in the post-monsoon season. Phosphate, ORP and F^- also form a cluster, while As and Fe are clustered together because of the involvement of Fe (hydr)oxides as the common source of both As and Fe. The cluster of Fe and As is close to the cluster of pH, HCO_3^- and SO_4^{2-}, indicating that alkaline environment promotes the evolution of more As, while SO_4^{2-} may act as a competitive anion for adsorption on the surface of Fe (hydr)oxides.

4.3.1.7. Speciation study

Speciation study can be used to analyse the potential of different aquatic phases or species to pollute the groundwater based on their saturation indices (SI) [13]. Speciation study was conducted on representative samples of the pre-monsoon and post-monsoon seasons [Table 4.9 and 4.10].

Table 4.9: SI values obtained by speciation modelling in the pre-monsoon season

	Samples											
Aqueous Phase	**T3**	**T9**	**T10**	**T14**	**T16**	**T42**	**T45**	**T50**	**T55**	**T56**	**T57**	**T63**
Aragonite	-1.58	-2.34	-1.88	-1.60	-0.93	-2.00	-2.76	-2.40	-0.48	-1.08	-0.37	-1.09
Arsenolite	-13.21	-13.40	-13.44	-12.97	-14.35	-14.31	-13.96	-13.71	-14.77	-12.69	-13.36	-13.15
As_2O_5	-36.41	-32.65	-31.76	-34.24	-36.59	-33.35	-36.47	-36.55	-36.14	-38.95	-33.48	-36.57
Calcite	-1.44	-2.19	-1.73	-1.46	-0.78	-1.85	-2.62	-2.25	-0.33	-0.94	-0.23	-0.94
Claudetite	-13.25	-13.44	-13.48	-13.01	-14.39	-14.35	-14.00	-13.75	-14.81	-12.73	-13.40	-13.19
Dolomite (disordered)	-3.53	-5.29	-4.38	-3.46	-2.25	-4.46	-5.87	-5.22	-0.88	NF	-0.98	-2.31
Dolomite (ordered)	-2.98	-4.74	-3.83	-2.91	-1.70	-3.91	-5.32	-4.67	-0.33		-0.43	-1.76
$Fe(OH)_2$ (am)	-5.09	NF	NF	NF	-4.74	NF	NF	-7.90	-4.34	-4.21	-3.67	-4.95
$Fe(OH)_2$(c)	-4.49	NF	NF	NF	-4.14	NF	NF	-7.30	-3.74	-3.61	-3.07	-4.35
Gypsum	-2.87	-3.07	-3.08	-2.85	-2.54	-2.99	-3.14	-3.25	-3.07	-3.48	-3.06	-2.55
Halite	-8.48	-8.36	-8.47	-8.00	-8.72	-8.50	-7.59	-8.27	-8.84	-3.13	-8.24	-8.08
Mirabilite	-9.95	-10.28	-9.78	-10.15	-10.75	-9.93	-9.18	-10.07	-10.16	-8.83	-9.68	-9.84
Siderite	-0.53	NF	NF	NF	-0.88	NF	NF	-3.03	-0.24	0.42	0.63	-0.29
$Fe(OH)_2.7Cl._3$(s)	NF	6.19	6.43	7.62	NF	6.18	5.80	NF	NF	NF	NF	NF
$Fe_2(SO_4)_3$(s)	NF	-30.99	-32.04	-31.91	NF	-33.81	-32.20	NF	NF	NF	NF	NF
$FeAsO_4$:$2H_2O$(s)	NF	-7.68	-6.79	-6.92	NF	-7.77	-10.02	NF	NF	NF	NF	NF
Ferrihydrite	NF	2.59	3.04	4.15	NF	2.85	2.16	NF	NF	NF	NF	NF
Ferrihydrite (aged)	NF	3.10	3.55	4.66	NF	3.36	2.67	NF	NF	NF	NF	NF
Geothite	NF	5.30	5.75	6.85	NF	5.56	4.87	NF	NF	NF	NF	NF

It is observed in our study that the As phases in the groundwater (Arsenolite, As_2O_5, Claudetite and $FeAsO_4$:$2H_2O$) are under-saturated in both the pre and the post-monsoon seasons. The SI values are lower in the post-monsoon season compared to the pre-

monsoon which could be due to the dilution effects of the precipitation. The mineral Siderite ($FeCO_3$) is in under-saturated state in the pre-monsoon samples. The condition reverses in the post-monsoon as the SI increases.

Table 4.10: SI values obtained by speciation modelling in the post-monsoon season NF here stands for 'not found'. am, c and s stand for amorphous, crystalline and solid respectively

	Samples											
Aqueous Phase	**T3**	**T9**	**T10**	**T14**	**T17**	**T18**	**T45**	**T51**	**T54**	**T55**	**T57**	**T63**
Aragonite	-0.39	-0.46	-0.62	-0.44	-1.15	-0.47	-0.75	0.45	-19.59	0.25	0.25	-0.72
Arsenolite	-17.19	-17.11	-13.42	-15.86	-18.40	-20.25	-19.77	-26.21	-7.66	-16.59	-13.12	-16.81
As_2O_5	-34.65	-33.59	-33.00	-33.62	-34.03	-33.55	-35.20	-38.71	-33.67	-35.95	-34.63	-38.77
Calcite	-0.25	-0.32	-0.48	-0.30	-1.00	-33.55	-0.61	0.60	-0.42	0.40	0.39	-0.58
Claudetite	-17.23	-17.15	-13.46	-15.90	-18.44	-20.29	-19.81	-26.25	-19.63	-16.63	-13.16	-16.85
Dolomite (disordered)	-1.07	-1.44	-1.61	-1.23	-2.51	-1.25	-1.82	0.70	-1.56	0.52	-0.01	-1.85
Dolomite (ordered)	-0.52	-0.89	-1.06	-0.68	-1.96	-0.70	-1.27	1.25	-1.01	1.07	0.54	-1.30
$Fe(OH)_2$ (am)	-2.71	NF	NF	-2.58	NF	NF	-2.35	-3.06	NF	-2.35	-1.81	-4.37
$Fe(OH)_2$(c)	-2.11	NF	NF	-1.98	NF	NF	-1.75	-2.46	NF	-1.75	-1.21	-3.77
Gypsum	-3.09	-1.90	-2.93	-3.22	-3.48	-3.26	-3.54	-25.02	NF	-3.14	-3.15	-3.17
Halite	-6.95	-8.46	-8.19	-7.75	-9.23	-7.94	-7.36	-3.20	NF	-8.38	-8.05	-8.02
Mirabilite	-9.84	-8.84	-9.71	-9.48	-11.93	-9.45	-9.11	-10.00	NF	-10.26	-9.36	-9.80
Siderite	0.93	NF	NF	1.07	NF	NF	0.80	-0.54	NF	1.05	1.71	-0.81
$Fe(OH)_2.7Cl.3$(s)	NF	8.63	7.95	NF	8.58	8.20	NF	NF	8.91	NF	NF	NF
$Fe_2(SO_4)_3$(s)	NF	-32.34	-34.65	NF	-36.45	-37.02	NF	NF	NF	NF	NF	NF
$FeAsO_4:2H_2O$(s)	NF	-5.09	-5.65	NF	-5.39	-5.55	NF	NF	-5.04	NF	NF	NF
Ferrihydrite	NF	5.66	4.80	NF	5.57	5.17	NF	NF	5.74	NF	NF	NF
Ferrihydrite (aged)	NF	6.17	5.31	NF	6.08	5.68	NF	NF	6.25	NF	NF	NF
Geothite	NF	8.36	7.51	NF	8.28	7.88	NF	NF	8.45	NF	NF	NF

Increase in SI points towards the tendency of minerals to precipitate out of the system. Siderite may precipitate in the post-monsoon and form coatings on primary minerals like Geothite and Ferrihydrite; decreasing their tendency to dissolve in the system [13, 58]. Iron (II) hydroxide [$Fe(OH)_2$] (both amorphous and crystalline) is more under-

saturated in the pre-monsoon compared to the post-monsoon indicating greater rates of dissolution in the post-monsoon. Aragonite, calcite and dolomite have higher SI in the post-monsoon indicating an approach towards saturation; this brings to light the elevated level of weathering and dissolution in post-monsoon compared to pre-monsoon. The As contamination in the groundwater of the area is likely to increase in the near future owing to the under-saturated level of the As bearing phases. At the same time primary minerals like Goethite and Ferrihydrite could act as sinks for both Fe and As in the groundwater. However prevalence of a reducing condition could lead to dissolution and further increase in the As level in the groundwater.

4.3.2. Impact of river proximity on arsenic and fluoride distribution in the BFP

In order to study the effect of proximity on the As distribution in the BFP, contour maps based on the As levels were prepared for the pre and the post-monsoon seasons. A seasonal aspect was chosen to observe the changes in As mobilization trends in the pre and the post-monsoon seasons. We could not prepare contour maps for F^- in the groundwater because the levels of F^- in the groundwater samples were very less. In many samples the F^- values were found to be below the detection limit of the instrument; in all other samples the F^- values were below 1.5 mgL^{-1} [16]. A close observation of the contour maps (Fig. 4.13a, b and 4.14a, b) reveals that As decreases with an increase in the distance from the river. The sediments which are brought down by the river contain minerals like arsenopyrite, which are the original sources of As [3, 6, 9, 59]. Sediments at closer proximity to the river are more recent and therefore may hold more As minerals. Another possibility is that the recent sediments are relatively less oxidized than the older sediments and therefore have more potential to release As in the groundwater. A third possibility is that the river is also involved directly in recharging and mobilizing the As in the groundwater, resulting in higher As closer to the river and lower levels away from it. From the extreme low levels of F^- detected in the flood plain region it can be assumed that the fluvial environment is not suitable for high groundwater F^- levels. The scatter plots, Fig 4.15a and b also show that As and proximity to the river are positively related while F^- did not appear to show any correlation with proximity.

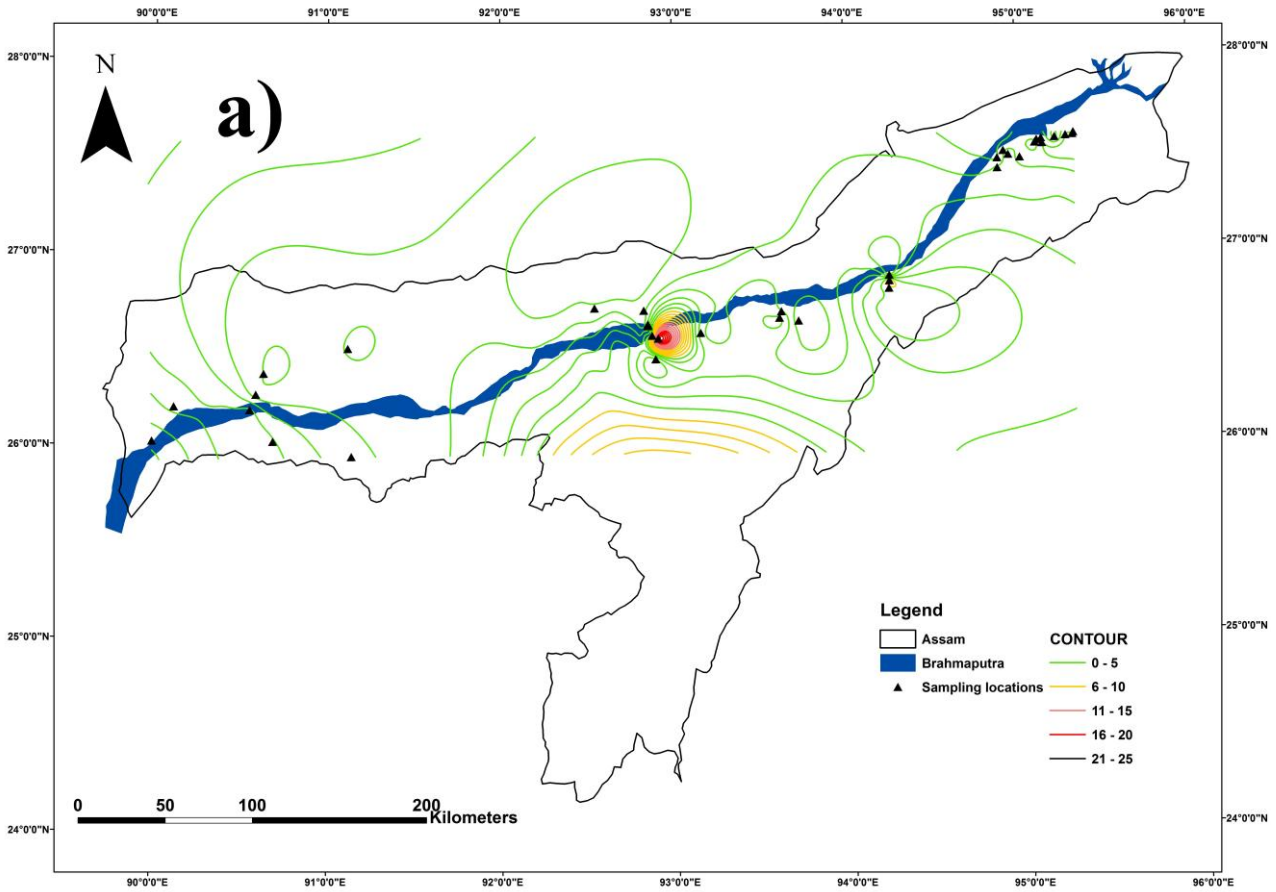

Figure 4.13(a): Contour map of As distribution in the pre-monsoon season in the BFP

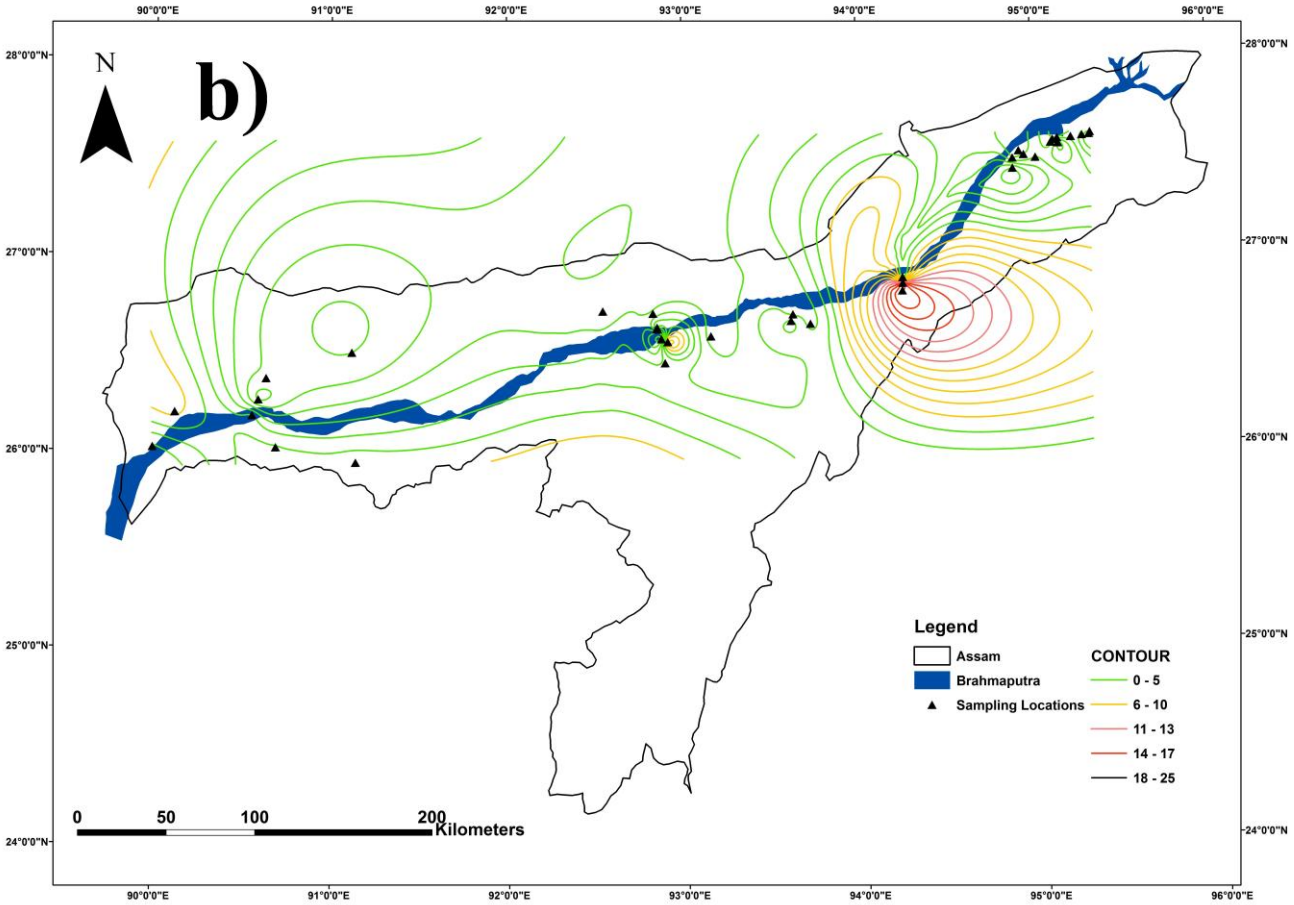

Figure 4.13(b): Contour map of As distribution in the post-monsoon season in the BFP

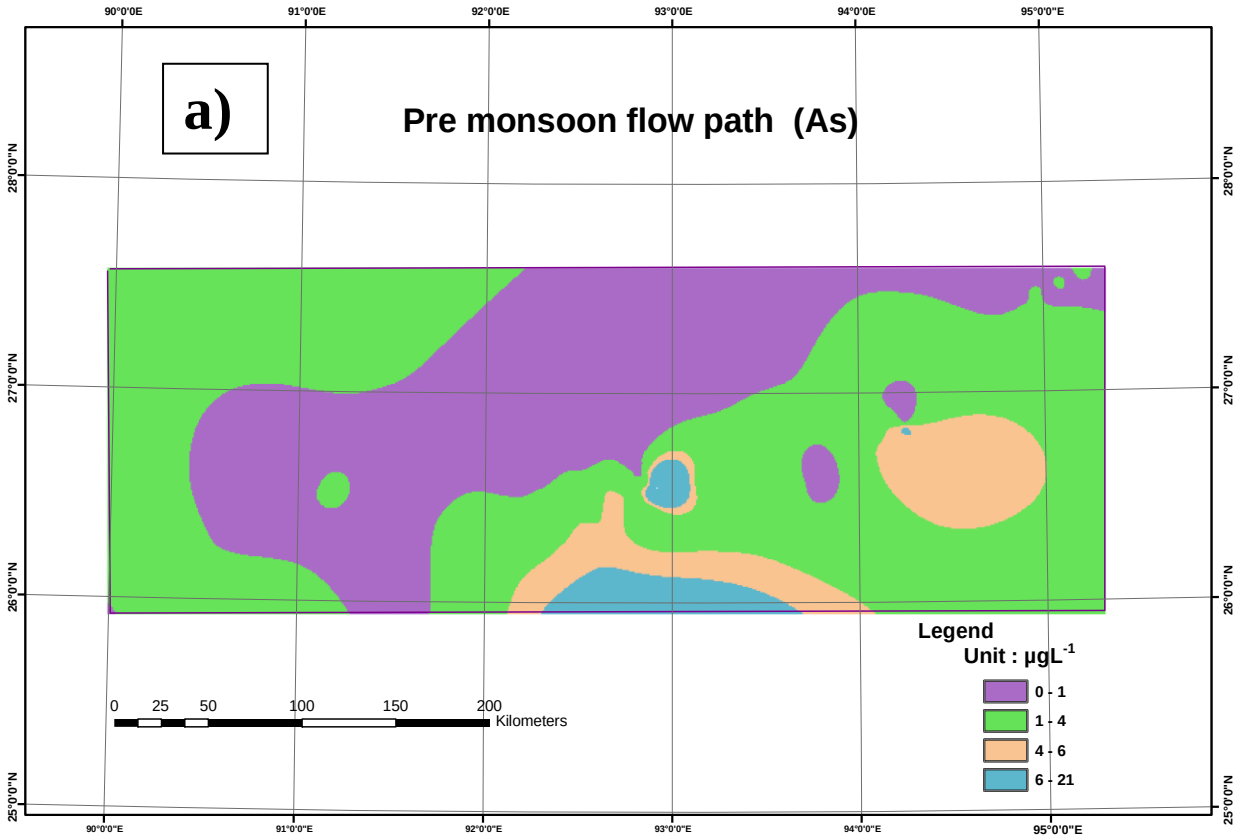

Figure 4.14(a): Arsenic recharge and distribution in pre-monsoon (Raster format)

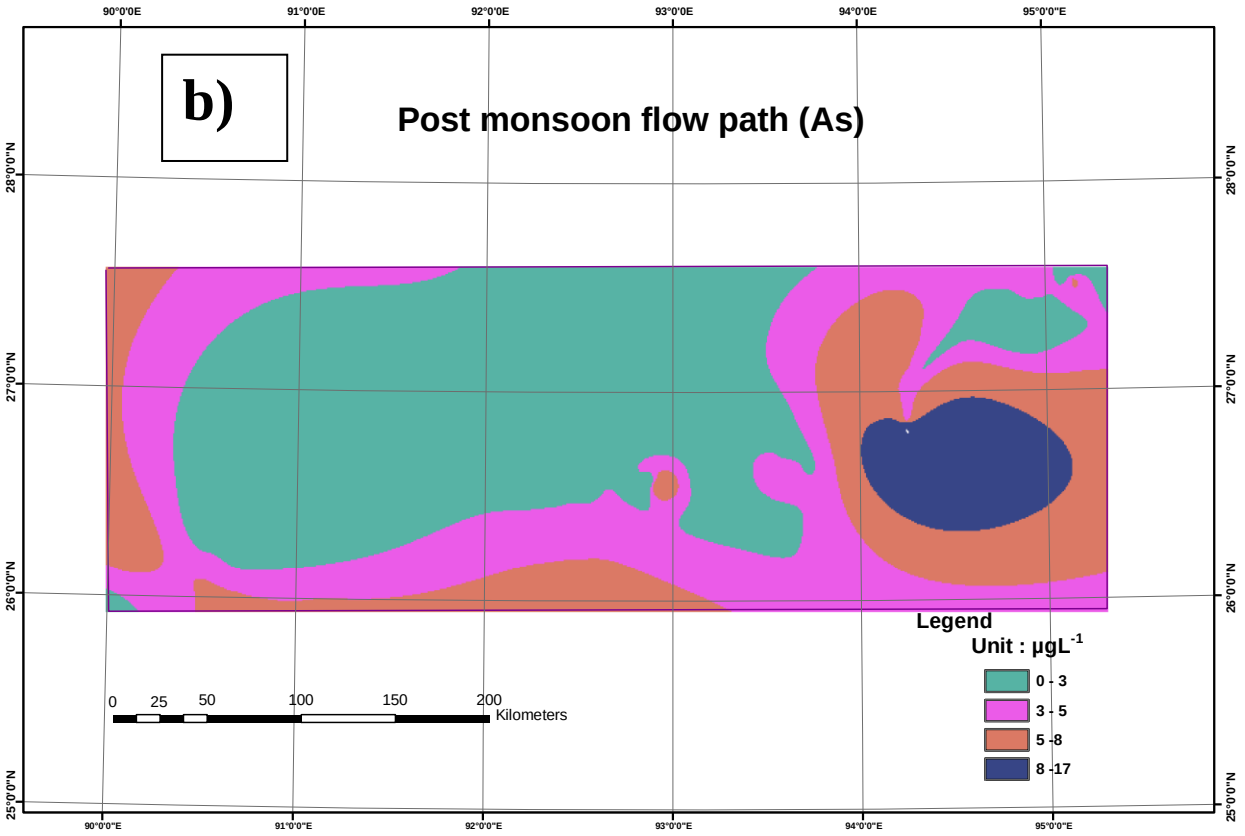

Figure 4.14(b): Arsenic recharge and distribution in post-monsoon (Raster format)

Fluoride has been detected in regions like the Nagaon and the Karbi Anglong districts of Assam. The F^- incidences in these regions appear to be localized in isolated patches where groundwater recharge appears to be low and the rock-water interaction is high. It is important to mention that both the above mentioned districts are rain shadow zones of Assam and on an average receive lower rainfall than rest of Assam which also means low recharge rates for the groundwater of these regions. The Karbi Anglong district where some of the highest groundwater F^- levels have been detected [18] is situated south of the BFP and has a different geology, comprising mainly of older hills.

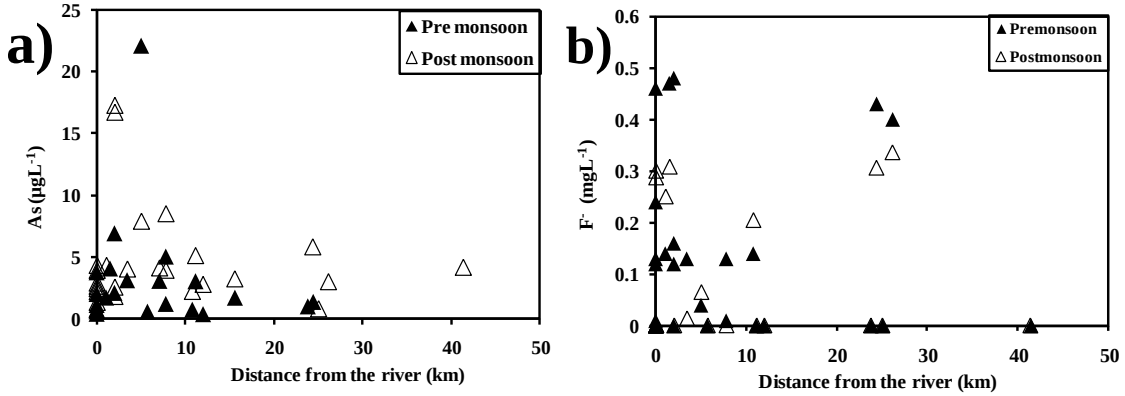

Figure 4.15: Influence of river proximity on (a) As and (b) F^- distribution in the BFP

The groundwater flow pattern depends on the surface topography to a large extent; it is a very important factor considering the fact that groundwater flow is also responsible for the transportation and circulation of different chemical and mineral species including pollutants. When it comes to pollutants, the groundwater flow path can be used to predict zones of recharge and discharge in larger areas with inter-connected aquifers. Contour mapping in both the pre and the post-monsoon seasons (Fig. 4.13a, b and 4.14a, b) show the presence of isolated hotspots of high As groundwater in the BFP. It is observed that there are at least two major recharge points for groundwater As in both the pre as well as the post-monsoon seasons. One is located close to the Kaliabor region in the Nagaon district in the south bank of river Brahmaputra (Fig. 4.13a, b and 4.14a, b). The other recharge point is close to the Majuli river island in the north of Jorhat district. In the rest of the BFP there appears to be mainly isolated recharge points

or hotspots rather than major recharge units. Also contour maps suggests that the overall As level may be higher in the pre-monsoon than in the post-monsoon season. Groundwater recharge due to precipitation in the post-monsoon season could lead to dilution of As level throughout the BFP, although on an average, groundwater As values are higher in the post-monsoon season in our study. The sudden increase in groundwater As levels in the Jorhat district in the post-monsoon could be due to mobilization of the highly mobile fractions of the As in the sediments which are easily replaceable by other anions like SO_4^{3-} and PO_4^{3-}. The different fractions of As have been discussed in the sixth chapter. It is also evident from the pre-monsoon contour map that the level of groundwater As increases towards the west or downstream of the river Brahmaputra. This could be due to an increase in the rate of sedimentation caused by the decrease in the velocity of the river downstream. As the source of the groundwater As is most likely to be the sediment brought down by the river, so higher rate of sedimentation would also mean higher As in the sediments.

4.3.3. Arsenic hydrogeochemistry in the Jorhat district

In order to gain a deeper understanding of the process of As mobilization in the BFP, an intensive sampling was carried out in the Jorhat district. This was done to have a better understanding of the local effects, land use patterns and anthropogenic influences on the process of As mobilization. As the F^- levels were found to be very low in BFP, therefore this section focuses only on the aspect of groundwater contamination due to As. The groundwater co-contamination aspects due to As and F^- has been discussed in greater depths in the succeeding chapters.

4.3.3.1. Summary of chemical parameters in the study area

The Table 4.11 give a summary of the different parameters in the groundwater of Jorhat district. pH was found in the range of 6.9-8.2 and 6.2-8.6 in monsoon (June 2013) and post-monsoon (January 2014) respectively, implying that conditions in the groundwaters of Jorhat is slightly acidic to alkaline. In the post monsoon the pH shifts more towards neutral. This is accompanied by an increase in the concentration of HCO_3^-

in the study area. This might be due to recharge of the groundwater during monsoon. Enrichment due to evaporation could be the cause of higher average value of EC at the start of the monsoon season. However the standard deviation is higher in the post-monsoon indicating more variability in the hydrochemical processes compared to monsoon season. It can also be further linked with the local variation in point sources, soil type, multiple aquifer system and other agriculture related activities in the area. Recharge of aquifers during post-monsoon season increases the DO levels (Table. 4.11).

Table 4.11: Descriptive statistics for monsoon and post-monsoon. The unit for TDS, DO, Na^+, K^+, Ca^{2+}, Mg^{2+}, H_4SiO_4, HCO_3^-, Cl^-, SO_4^{2-}, PO_4^{3-} and Fe is mgL^{-1}, while the units for EC, ORP and As are µS/cm, mV and μgL^{-1} respectively. ND stands for "not detectible"

	Monsoon			Post-monsoon		
Parameters	**Range**	**Average-SD**	**Co-efficient of Variance**	**Range**	**Average-SD**	**Co-efficient of Variance**
pH	6.93- 8.20	7.55-0.36	0.04	6.25-8.60	7.15-0.46	0.06
EC	98-516	262-88.20	0.33	126-471	258-75.80	0.29
TDS	49-259	127-43.70	0.34	63-235	129-37.20	0.28
ORP	-144-109	96.0-44.80	0.50	-130-75.40	-41.10-48.80	-1.2
DO	0.20-2.55	0.67-0.57	0.85	0.64-7.75	2.66-1.65	0.62
Na^+	4.06-106	27.9-22.0	0.78	7.48-60.80	21.20-11.70	0.55
K^+	1.31-9.23	2.39-1.55	0.64	1.03-7.59	2.29-1.26	0.55
Ca^{2+}	2.68-18.5	6.97-3.99	0.50	1.43-37.20	5.70-7.32	1.20
Mg^{2+}	BDL-16.6	5.93-3.55	0.60	1.780-16.50	5.96-3.03	0.51
H_4SiO_4	BDL-38.4	13.6-9.20	0.67	3.81-16.6	9.75-3.19	0.32
HCO_3^-	70-470	261-121	0.46	100-360	212-58.0	0.27
Cl^-	19.8-201	61.60-33.5	0.54	28.40-76.60	42.0-10.30	0.24
SO_4^{2-}	17.5-135	58.40-29.40	0.50	8.25-88.3	21.90-15.80	0.72
PO_4^{3-}	0.06-0.55	0.17-0.130	0.77	0.02-0.44	0.13-0.12	0.93
Fe	0.11-18.6	4.07-5.01	1.23	6.25-18.30	4.08-4.08	0.99
As	0.21-44.6	6.51-10.80	1.66	0.19-73.0	13.40-17.90	1.33

TDS is not exceptionally high. It is within the permissible range of $\leq$500 mgL^{-1}, established for total dissolved solids (TDS) in drinking water by WHO [16]. There is no significant difference in the TDS values for monsoon and post-monsoon. The ORP is found to be mostly negative in the study area for both monsoon and post-monsoon; this

indicates the predominance of a reducing condition in the aquifers of Jorhat. Oxidizing conditions were found to be more prevalent in the monsoon season than the post-monsoon season. This was because the sampling was conducted at the beginning of monsoon season when there was still sufficient air space or under-saturation in the aquifers leading to the occurrence of isolated incidences of oxidation. Low average value of HCO_3^- in the post-monsoon can be due to the dilution by rainwater in post-monsoon.

4.3.3.2. Graphical representation of hydrochemical data

The Piper plot [42, 60, 61] have been used for initial investigation of the groundwater in the Jorhat district. According to the Piper plot, most of the samples in monsoon as well as the post-monsoon season can be classified under Na^++K^+-HCO_3^-+CO_3^- category (Fig. 4.16). This is indicative of silicate and carbonate weathering in the study area. The number of samples which fall under this facie is higher in the post-monsoon season implying higher rates of silicate, and carbonate weathering and dissolution in the post-monsoon due to precipitation. The recharge of the aquifers is apparent in the post-monsoon season. The groundwater samples are more spread and there is a shift towards HCO_3^- water in the post-monsoon. This again indicates the importance of carbonate weathering in the post-monsoon season. The Durov plot is similar to the Piper plot but it has the additional features of pH and TDS. Similar results were obtained in the Durov diagram (Fig 4.17) as the water type in both the monsoon and post-monsoon seasons is mostly Na^++K^+-HCO_3^-+CO_3^-. This, as mentioned above, is indicative of silicate and carbonate weathering. Most of the samples including those with high levels of As have a pH > 7 (Fig. 4.17), indicating that increasing alkalinity can induce weathering, dissolution and enhances As level in the groundwater. It can be observed from the plots that the pH of the groundwater samples has more variance or spread in the post-monsoon season; while in the monsoon the pH values are more stable. This could be due to the influence of infiltrating water. Also it is seen that in both the seasons the range of TDS is similar, but in the post-monsoon season a marked increase in TDS is visible in many of the samples. This implies more weathering and dissolution of minerals in the post-monsoon due to precipitation. The Scholler diagram also shows that

$HCO_3^-+CO_3^-$ type facie is the most dominant among anions in both the monsoon as well as the post-monsoon (Fig. 4.18 and 4.19), while Na^++K^+ is the most dominant cation phase in both the monsoon and the post-monsoon seasons. Silicate weathering and carbonate weathering are the most dominant hydrochemical process in the study area. It is observed that samples with high As are associated with HCO_3^- and high Na^++K^+ phases in both monsoon and post-monsoon. Thus it can be implied that an alkaline environment is suitable for As enrichment. It is also seen that in the monsoon season a few high As level samples are associated with high SO_4^{2-}, indicating towards the occurrence of isolated incidences of pyrite oxidation in some of the aquifers. Thus pyrite oxidation doesn't appear to have a widespread occurrence in the area. A similar relation between As and SO_4^{2-} is lacking in the post-monsoon season.

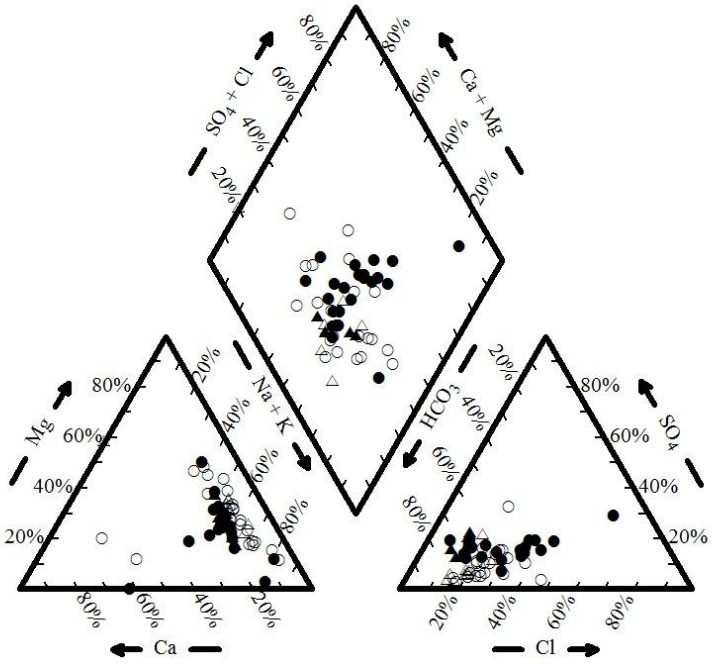

Figure 4.16: Piper plot showing the samples of monsoon and post-monsoon. The black dots and the hollow dots represent monsoon and post-monsoon samples respectively, while the black and hollow triangles represent samples with As level > 10µgL^{-1} in monsoon and post-monsoon respectively

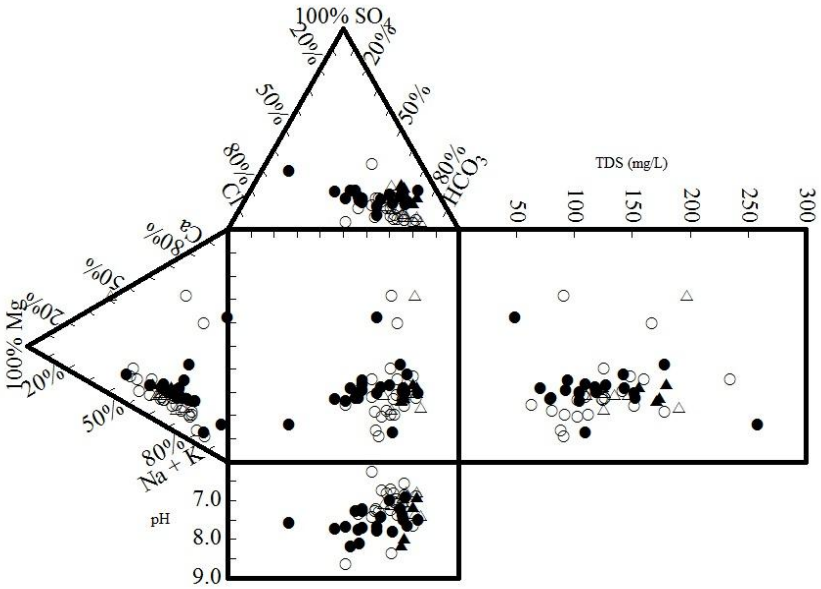

Figure 4.17: Durov plot showing the samples of monsoon and post-monsoon. The black dots and the hollow dots represent monsoon and post-monsoon samples respectively, while the black and hollow triangles represent samples with As level > 10µgL^{-1} in monsoon and post-monsoon respectively

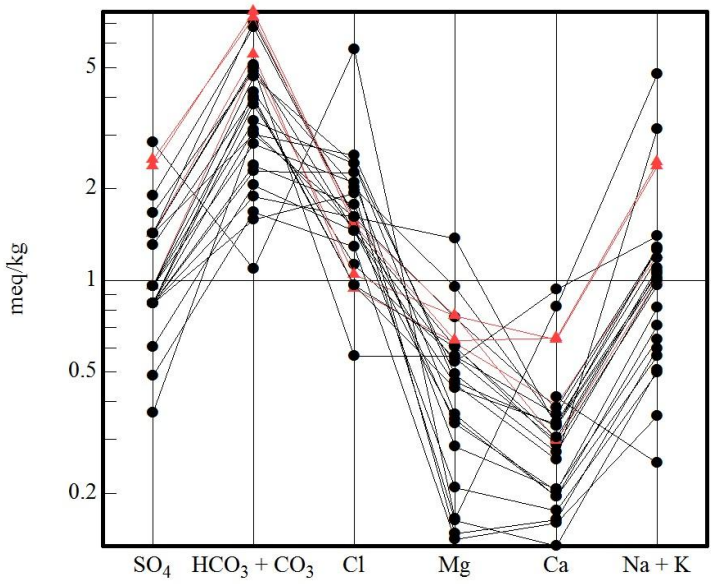

Figure 4.18: Schoeller diagram for monsoon season, the red triangles represent samples with with As level > 10µgL^{-1}

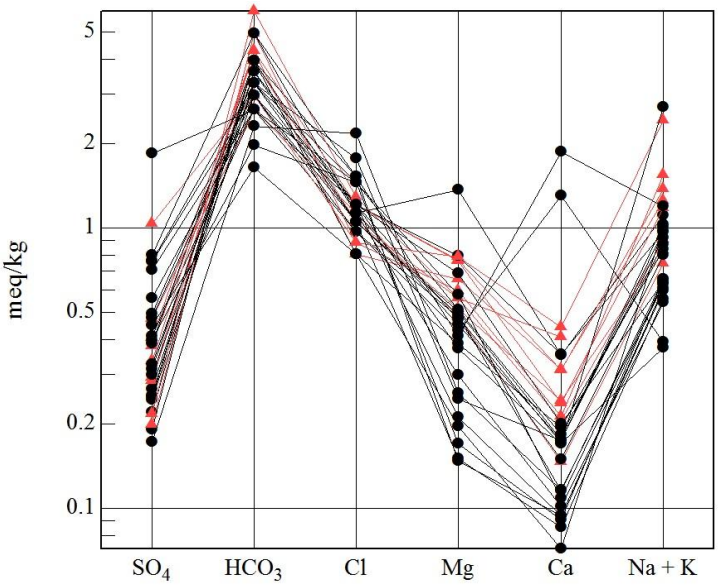

Figure 4.19: Schoeller diagram for post-monsoon season, the red triangles represent samples with with As level > 10µgL^{-1}

4.3.3.3. Hydrochemistry of the study area

In Jorhat, all the collected groundwater samples are influenced by rock-water interaction in both the monsoon and post-monsoon seasons (Fig. 4.20a and b) [43]. Silicate and carbonate weathering are reported to be the two most dominant hydrochemical processes occurring in any natural groundwater system [41]. The contributions due to silicate or carbonate weathering can be assessed by a number of hydrochemical plots, some of which have been used in our study. The following section explains the weathering processes based on these plots. In our study, the Tz^+ versus Na+K plot shows that: most of the sampling points fall along the $Na+K=0.5Tz^+$ line (Fig. 4.21a). This line is indicative of silicate weathering; thus silicate weathering is an important process in both the monsoon and the post-monsoon seasons [49]. A few samples in the monsoon fall below the $Na+K=0.5Tz^+$ which can be due to incidences of ion exchange between Na^+ and Ca^{2+} [62, 63]. Silicate weathering is more dominant than carbonate weathering, this can be observed from the Tz^+ versus Ca+Mg plot (Fig. 4.21b); here most of the samples in both the seasons lie on the $Ca+Mg=0.5Tz^+$ line [49]. A few incidences of reverse ion exchange can also be observed in the post-monsoon.

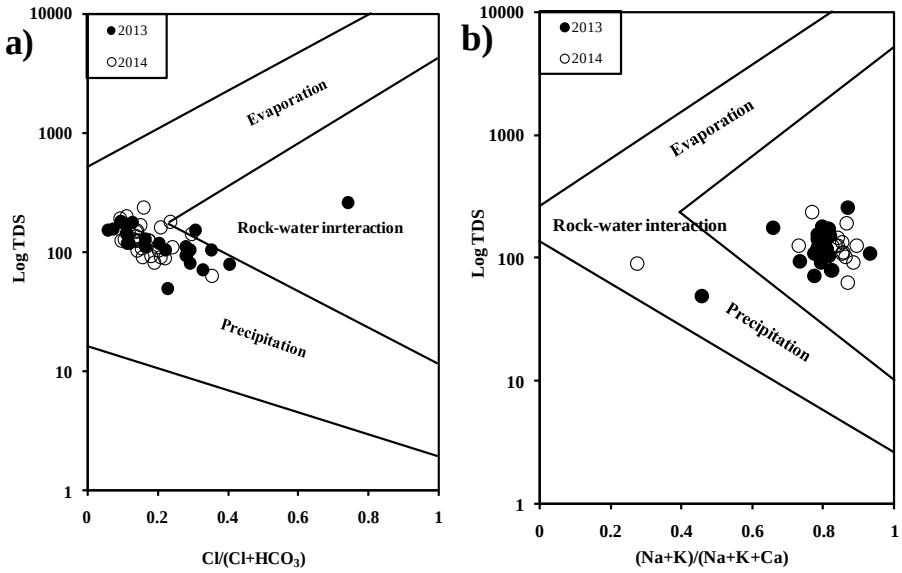

Figure 4.20: Gibbs plots for (a) monsoon and (b) post-monsoon

Carbonate weathering results in release of HCO_3^- into the groundwater. Therefore the plot of HCO_3^- versus Ca^{2+} can be used to study the occurrence of carbonate weathering in the groundwater of the study area. In our study, it is seen that almost all the samples in monsoon as well as the post-monsoon seasons lie above the 1:1 line (Fig. 4.21c), indicating an excess of HCO_3^- over Ca^{2+}. This is due to carbonate (calcite) weathering in the aquifers [49]; an excess of Ca^{2+} would have meant that Ca^{2+} was released due to silicate weathering rather than carbonate weathering. The Ca^{2+}+Mg^{2+} versus HCO_3^- +SO_4^{2-} plot can be used to identify hydrochemical processes like calcite, dolomite and gypsum dissolution. It can also point to the dominance of ion exchange and reverse ion exchange in the aquifer. If the groundwater samples are plotted along the 1:1 line, then various phases associated with Ca^{2+} and Mg^{2+} like calcite, dolomite and gypsum could be their sources. If the points lie towards SO_4^{2-}+HCO_3^- i.e., towards the right of the 1:1 line then ion exchange is the dominant hydrochemical process. If the points fall on the left side of the 1:1 equiline then reverses ion exchange is the main process [41, 52, 53]. In our study it was found that in both the monsoon as well as the post-monsoon seasons the groundwater samples are plotted below the 1:1 (Fig. 4.21d) line indicating the presence of ion exchange processes [49].

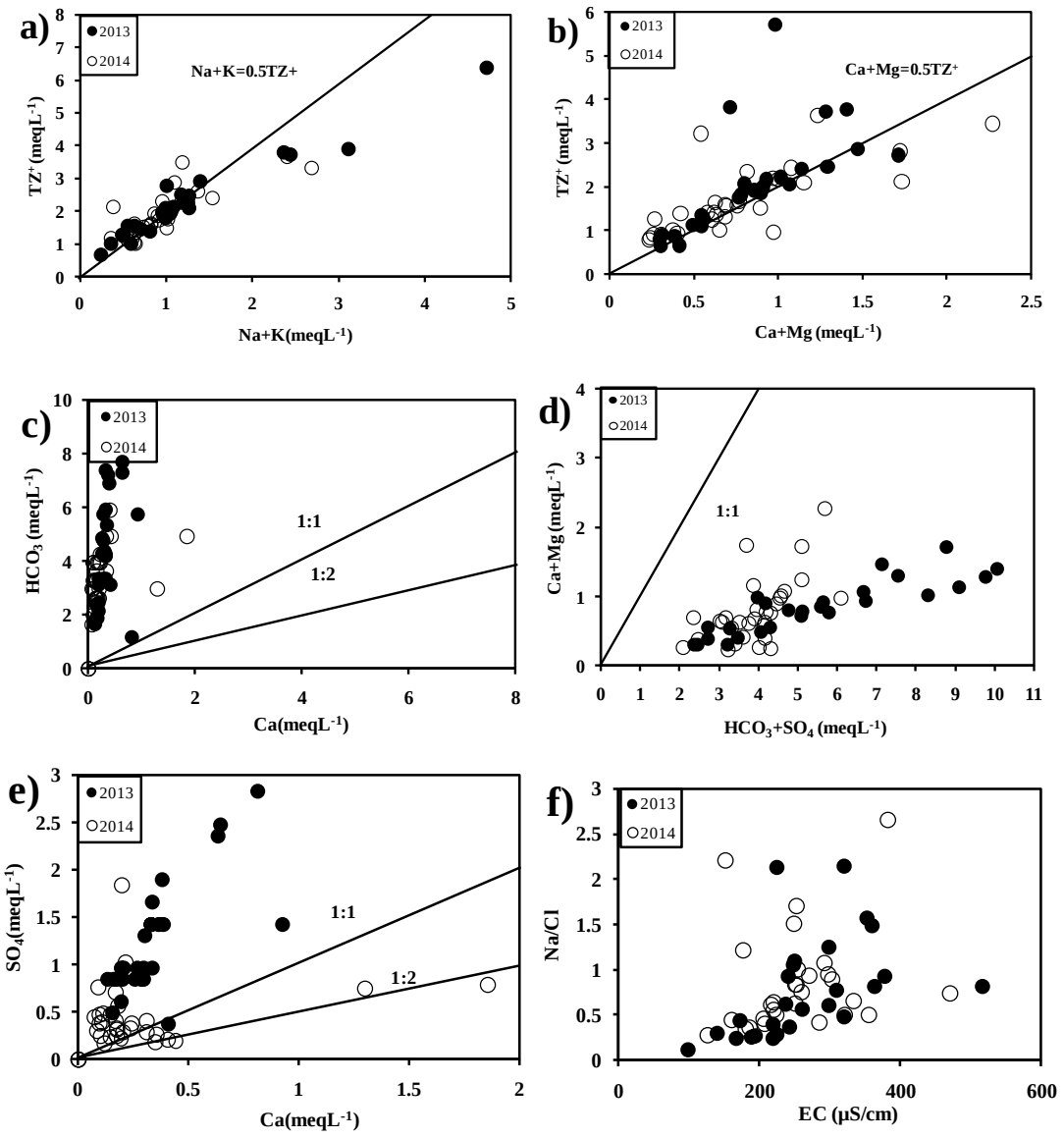

Figure 4.21: Scatter plots representing the hydrochemical trends (a). Tz^+ vs (Na+K), (b) Tz^+ vs (Ca+Mg), (c) HCO_3 vs Ca, (d) (Ca+Mg) vs (HCO_3+SO_4), (e) SO_4 vs Ca and (f) (Na/Cl) vs EC

Ion exchange and calcite precipitation are processes which can remove Ca^{2+} from the groundwater system. The plot of SO_4^{2-} versus Ca^{2+} shows that there is an excess of SO_4^{2-} over Ca^{2+} in the study area as seen from the figure 4.21e, this could be due to removal of Ca^{2+} by calcite precipitation [63]. This trend is true for the monsoon samples. In the post-monsoon, many samples lie on the 1:1 line and some also lie on the 1:2 line. Samples on the 1:1 indicate gypsum or anhydrite dissolution; while those lying

on the 1:2 line indicate carbonate phase weathering [49]. Evaporation is an important process, the occurrence of which can be assessed by the Na/Cl versus EC plot [41]. The Na/Cl ratio would remain unchanged with an increase in EC if evaporation is the dominant process [41, 64]. Silicate weathering is the main process if Na/Cl increases with EC [41, 44], while decrease in this ratio would mean an enhancement in the salt dissolution [41]. In the present study it is observed that the Na/Cl ratio remains < 1 in most samples for monsoon as well as post-monsoon indicating the presence of salt dissolution (Fig. 4.21f). Reduction in Na^+ levels could be due to ion exchange processes in the study area [41]. A few samples in both the monsoon and post-monsoon season have Na/Cl ratio close to 1 depicting halite dissolution process (Fig. 4.21f). An increase in Na/Cl ratio with the EC value in samples of both the seasons is observed and therefore silicate weathering appears to a dominant process in the samples with higher EC levels (Fig. 4.21f).

4.3.3.4. Distribution of arsenic

The highest level of groundwater As in Assam was recorded by Singh [18] in Jorhat district, where the highest recorded level of groundwater As was 657 μgL^{-1}. In the present study, such high values of As was not recorded and the highest values of groundwater As were 44.68 μgL^{-1} and 73 μgL^{-1} in the monsoon and the post-monsoon seasons respectively. Which are still much higher than the WHO [16] prescribed limit for As in drinking water i.e., 10 μgL^{-1}. The above observation shows that As in groundwater is distributed in patches, wells with very high As levels were found to be located near wells which had As within the WHO prescribed limit of 10 μgL^{-1} for drinking water. Therefore uniformity in high groundwater As is lacking in the district. Higher levels of As (>10 μgL^{-1}) were recorded more in the post-monsoon season than in the monsoon season. This could be due to infiltration of rain water in to the aquifers leading to expulsion of air and thereby leading to the development of a more reducing condition in the post-monsoon. An increase in pH generally causes various surfaces like Fe (hydr)oxides to accumulate a net negative charge [57]. Since both the III as well as the V forms of As exists in groundwater mainly as oxyanions therefore their affinity for such surfaces decreases with an increase in pH [57] ultimately leading to mobilization

of As. The same phenomenon appears to hold true in our study area as a higher pH seems to favour As release in the groundwater of the study area in both the monsoon as well as post-monsoon seasons (Fig. 4.22a). Higher values of As have been recorded at elevated levels of HCO_3^- (Fig. 4.22b), thus an increase in alkalinity could lead to subsequent increase in As in the groundwaters of Jorhat. A reducing condition is dominant in the groundwater samples collected from the Jorhat district. This is evident from the negative ORPs (Fig. 4.22c) recorded in most of the above mentioned samples. An inverse relation is observed between As level in groundwater and the ORP (Fig. 4.22c); thus a reducing condition favours the release of As in the groundwater. The phenomenon of reductive hydrolysis of iron (hydr)oxides as the mobilizing process for As in groundwater has already been discussed in the introduction section and could have an influence in the As behaviour in the groundwater of the study area. In order to investigate the role of Fe, the As versus Fe graph was plotted and it was observed that As and Fe did not share a positive relationship (Fig. 4.22d), instead a negative relationship was observed between the two. If reductive dissolution of Fe (hydr)oxides is the process of As mobilization, then a positive relation would be observed between the two. Many researchers have reported that either As or Fe may behave non-conservative in a groundwater system [13, 14, 65]. In our study too, Fe may be precipitated to phases like siderite ($FeCO_3$) as soon as it is released into the groundwater which could account for the negative correlation of Fe and As in the study area. Another important pathway for As mobilization is the oxidation of sulphides like pyrite and arsenopyrite. In our study a positive relation between As and SO_4^{2-} has been found in the monsoon, while no relation is observed in the post-monsoon season (Fig. 4.22e). Since the monsoon samples were collected at the beginning of the rainy season therefore the condition was still sufficiently oxidizing in some aquifers due to lowering of water levels and intrusion of oxygen resulting in pyrite oxidation in some isolated aquifers. A negative relation is also observed between As and H_4SiO_4 (Fig. 4.22f) in both the seasons. This could be due to the fact that silica may act as a competitive anion and may replace As from the solution [6]. This could also mean the reverse, i.e., low silica may mean that As has replaced it.

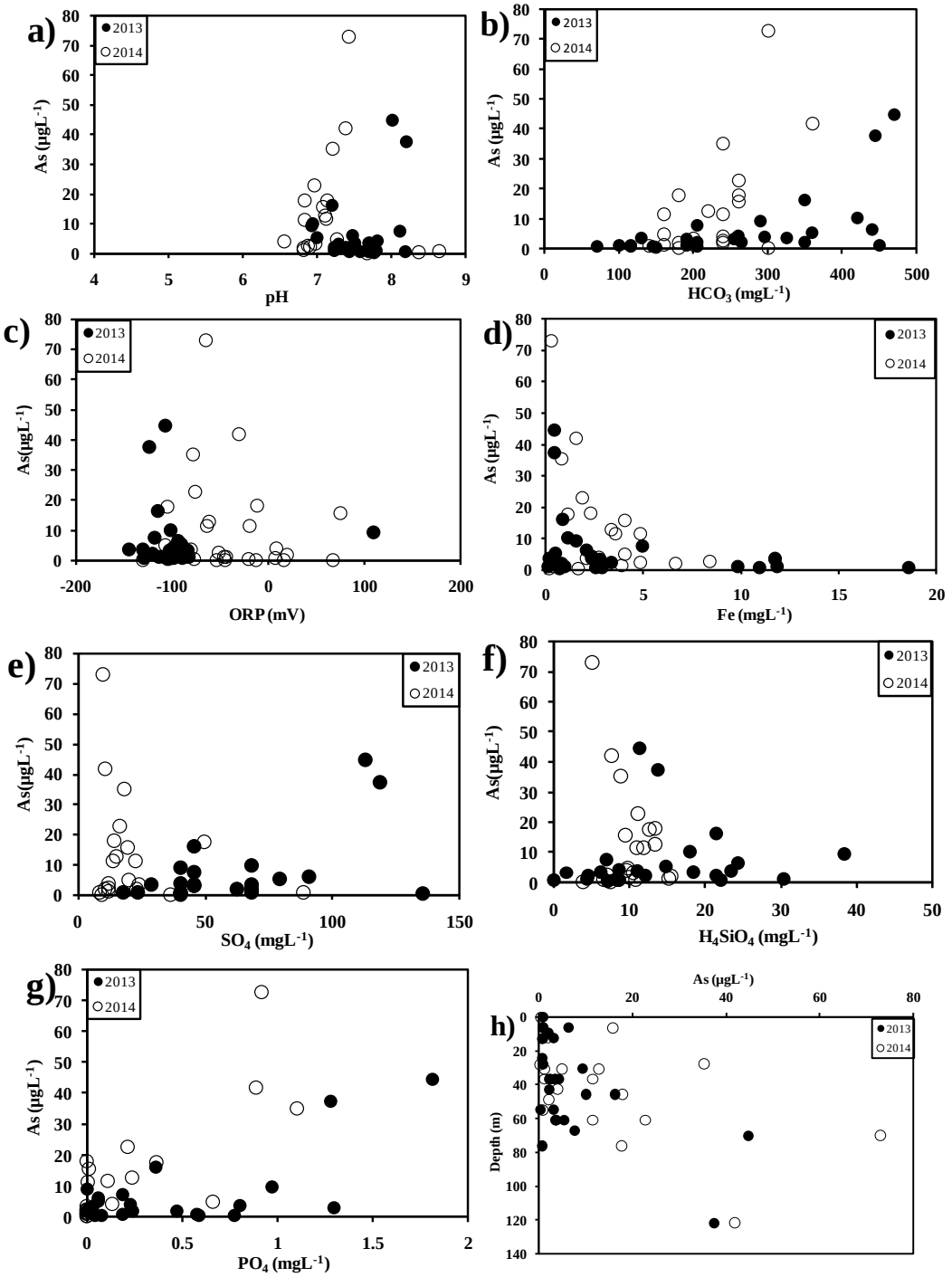

Figure 4.22: Hydrochemistry and behaviour of As with. (a) pH, (b) HCO_3, (c) ORP, (d) Fe, (e) SO_4^{2-}, (f) H_4SiO_4, (g) PO_4 and (h) depth

Phosphate and As may share a strong relation when their source is anthropogenic. Use of phosphate fertilizers may enhance the mobility of As in groundwater [66]. Arsenic and PO_4^{3-} could share similar adsorption sites on various minerals and substrates, which

on weathering and dissolution could co-release both the contaminants resulting in their relationship (Fig. 4.22g). The Jorhat district is an important tea producing district of Assam and depends heavily on phosphate fertilizer usage; however the level of PO_4^{3-} in the groundwater of the region has been found to be very low. Therefore it is unlikely that anthropogenic fertilizers would have much effect on As mobilization in the region.

It was observed in both monsoon and post-monsoon seasons that high As was found at greater depths i.e., in aquifers of medium depths which has a depth range of 60-90 m (Fig. 4.22h). In many studies however it has been found that high As was more profound at shallow depths [57, 67], the groundwater could remain under-saturated with respect to As till greater depths in our study. Kim et al [57] have reported that at greater depths sulphide reduction could lead to loss of As from the groundwater system, because at greater depths, the ORP becomes much more reducing than is needed for reductive dissolution of Fe (hydr)oxides. Geological exploration of the Jorhat district reveals that clay beds are profound in the region up to depths of 103 m [68]. Clay fractions are known to hold higher amounts of organic matter and can also provide more surface area for Fe (hydr)oxides [6] and could be responsible for higher As at greater depths in this region. Observation of the contour maps in the previous part shows that the entire Jorhat region is an As hotspot (Fig. 4.13b and 4.14b). The Jorhat region has higher rates of sedimentation especially in and around the Majuli river island which is the largest river island in the world. Since sediments with As bearing minerals could be the original or primary sources of As, therefore higher rates of sedimentation could be associated with higher groundwater As.

4.3.3.5. Statistical analysis

4.3.3.5.1. Correlation analysis

In our study, EC showed good correlation with TDS, Na^+, SO_4^{2-} and Ca^{2+} in the monsoon season (Table. 4.12). It is understandable that dissolved solids account for all the dissolved inorganic and organic fractions in groundwater, therefore a good correlation is observed between EC and TDS. Weathering and dissolution is an important process in the groundwater of the study area. Weathering of various salts like

gypsum ($Ca_2SO_4.2H_2O$) and mirabilite ($Na_2SO_4.10H_2O$) could account for the positive correlation between the EC, Na^+, SO_4^{2-} and Ca^{2+} in the monsoon. Total dissolved solids also shares positive correlation with Na^+, SO_4^{2-} and Ca^{2+} (Table. 4.12) in the monsoon season. The reason could be the same as explained for EC, weathering of various salts could be the cause of these positive correlations. Bicarbonate shares a positive relation with As and Mg in the monsoon (Table. 4.12), while a negative correlation is observed with Fe, an increase in alkalinity could lead to enrichment of As in the groundwater. Carbonate weathering and dissolution being an important process in the study area could account for the positive relation between Ca^{2+} and HCO_3^-. Na^+ has positive correlations with Cl^-, SO_4^{2-} and Ca^{2+} (Table. 4.12) in the monsoon, halite dissolution could be the cause of the positive relation between Na^+ and Cl^-. Weathering of various minerals like gypsum and mirabilite could account for correlation between Na^+, SO_4^{2-} and Ca^{2+}. Sulphate shares a positive correlation with As in the monsoon (Table. 4.12), which could be due to As release from oxidation of sulphide minerals like pyrites and arsenopyrites. Arsenic and phosphorus form similar anions in groundwater which can share similar adsorption sites and may be released when dissolution of such substrates occur. This could explain the positive relation between As and PO_4^{3-} in the groundwater. Anthropogenic input of phosphate fertilizers like monoammonium phosphate (MAP) or monocalcium phosphate (MCP) could also account for some minor correlation between As and PO_4^{3-}. Magnesium and Fe share a negative correlation (Table. 4.12) in the monsoon, which could be due to competition for adsorption sites between them. In the post-monsoon EC shares a positive correlation with HCO_3^-, As, TDS and Mg^{2+} (Table. 4.13). The effect of carbonate weathering and dissolution due to precipitation are prominent in this season accounting for the positive correlation between EC and HCO_3^- (Table. 4.13). The dissolution process also affects the mobilization of As in the groundwater. Bicarbonate shares a good correlation with As and TDS in the post-monsoon (Table. 4.13). The former could be due to positive influence of alkalinity on As mobilization while carbonate weathering could account for the latter. Arsenic shares positive correlations with Na^+, TDS and PO_4^{3-} (Table 4.13). Both As and PO_4^{3-} behave similarly and can share similar adsorption sites. During post-monsoon season, dissolution and weathering of various substrates which bind both As and PO_4^{3-} could be the cause of positive relation between As and PO_4^{3-}(Table. 4.13).

Table 4.12: Correlation matrix for monsoon

Parameters	pH	DO	ORP	EC	TDS	Na^+	K^+	Ca^{2+}	Mg^{2+}	HCO_3^-	Cl^-	SO_4^{2-}	PO_4^{3-}	H_4SiO_4	Fe
DO	-0.13														
ORP	-0.42	0.01													
EC	-0.18	-0.18	-0.08												
TDS	-0.20	-0.16	-0.05	**0.99**											
Na^+	0.13	-0.14	0.02	**0.73**	**0.75**										
K^+	-0.09	-0.16	-0.03	0.37	0.39	0.25									
Ca^{2+}	-0.02	0.01	0.04	**0.74**	**0.75**	**0.63**	**0.76**								
Mg^{2+}	-0.23	0.01	0.03	0.41	0.38	0.11	-0.04	0.19							
HCO_3^-	-0.14	0.13	0.06	0.40	0.39	0.15	0.10	0.39	**0.82**						
Cl^-	0.16	-0.29	-0.08	0.39	0.40	**0.57**	0.25	0.31	-0.29	-0.41					
SO_4^{2-}	0.09	-0.12	-0.11	**0.8**	**0.82**	**0.76**	0.29	**0.74**	0.39	0.48	0.44				
PO_4^{3-}	0.17	0.29	-0.08	0.32	0.34	0.36	-0.09	0.35	0.12	0.35	-0.03	0.43			
H_4SiO_4	-0.32	-0.15	0.47	0.06	0.04	-0.17	-0.36	-0.18	**0.64**	0.48	-0.37	-0.04	-0.04		
Fe	0.13	-0.27	-0.11	0.03	0.04	0.18	0.02	-0.09	-0.53	-0.69	**0.53**	0.02	-0.18	-0.41	
As	0.29	-0.05	-0.03	0.39	0.38	0.33	-0.06	0.39*	0.32	**0.60**	-0.15	**0.55**	**0.69**	0.11	-0.30

Table 4.13: Correlation matrix for post-monsoon

Parameters	pH	DO	ORP	EC	TDS	Na^+	K^+	Ca^{2+}	Mg^{2+}	HCO_3^-	Cl^-	SO_4^{2-}	PO_4^{3-}	H_4SiO_4	Fe
DO	0.14														
ORP	-0.15	0.18													
EC	-0.06	-0.35	-0.39												
TDS	-0.05	-0.35	-0.38	**0.99**											
Na^+	-0.01	-0.07	0.10	0.19	0.25										
K^+	0.06	-0.03	0.20	0.35	0.36	0.10									
Ca^{2+}	0.38	-0.03	0.01	0.24	0.24	0.04	**0.72**								
Mg^{2+}	0.13	-0.14	-0.24	**0.53**	**0.53**	0.31	-0.08	0.12							
HCO_3^-	-0.10	-0.18	-0.01	**0.55**	**0.54**	0.28	0.33	0.36	0.44						
Cl^-	0.27	-0.01	0.31	-0.06	-0.06	-0.21	0.40	0.03	-0.26	-0.11					
SO_4^{2-}	0.09	0.04	0.06	-0.05	-0.04	-0.01	0.14	0.20	-0.03	-0.32	-0.02				
PO_4^{3-}	0.12	-0.35	-0.25	0.37	0.36	0.26	0.25	0.29	0.14	0.46	-0.14	-0.05			
H_4SiO_4	-0.44	0.10	-0.18	-0.15	-0.16	-0.17	-0.30	-0.39	-0.14	-0.07	-0.24	0.05	-0.19		
Fe	-0.46	-0.01	0.18	-0.13	-0.14	-0.28	0.02	-0.34	-0.44	-0.10	0.21	-0.15	-0.37	0.02	
As	-0.02	-0.32	-0.11	**0.64**	**0.64**	**0.81**	0.37	0.12	0.25	**0.59**	-0.21	-.020	**0.79**	-0.27	-0.41

Use of phosphate fertilizers in the tea gardens can also be one of the reasons of this relationship, though it is unlikely to occur on such a large scale as the level of phosphate detected in the groundwater is very low in our study. Calcium shares a positive correlation with K^+; polyhalite and associated salt dissolution could be the cause of this relationship. Carbonate weathering is more prominent in the post-monsoon and could account for Mg^{2+} release and therefore could be the reason for the positive relation between TDS and Mg^{2+} (Table. 4.13).

4.3.3.5.2. Multivariate statistical analysis

Table 4.14 PCA loadings of the various parameters in the monsoon and the post-monsoon seasons.

Parameters	Monsoon				Post-monsoon			
	PC 1	PC2	PC3	PC4	PC1	PC2	PC3	PC4
pH			-0.83					0.57
TDS	0.92					0.62		
EC	0.91					0.64		
ORP			0.79			-0.86		
DO								0.76
Na	0.88							0.56
K				0.88			0.83	
Ca	0.77			0.53			0.90	
Mg		0.83				0.51		
HCO_3		0.90			0.64			
Cl		-0.65						
SO_4	0.91							
PO_4					0.72			
H_4SiO_4		0.61				0.52		0.56
Fe		-0.81						
As	0.52				0.92			
Variance (%)	33.5	21.6	12.05	8.67	36.87	15.43	10.15	7.37

I. Principal components analysis

In our study we obtained four principal components (PCs) in both the monsoon as well as the post-monsoon seasons using Varimax rotation and Kaiser Normalization (Table. 4.14). The 3D loading plots of the first three components of both the seasons are

represented in figures 4.23a and b**,** and can be used to interpret the closeness between each parameter. In the monsoon, PC 1 has 33.46 % variance and high loadings from TDS, EC, Na^{+}, Ca^{2+}, SO_4^{2-} and medium loading from As. Oxidation of sulphides could act as a source of groundwater As resulting in positive loadings of both As and SO_4^{2-} in this PC. Arsenic appears to be associated with the above mentioned phases and is released during weathering and dissolution of those phases. PC 2 is represented by Mg^{2+}, H_4SiO_4, HCO_3^{-}, and silicates as well as carbonate weathering are the controlling processes in this PC. Iron may be selectively replaced by cations like Ca^{2+} accounting for its negative loading. ORP has a positive loading on PC 3; this component could represent the reducing condition prevalent in the region. K^{+} and Ca^{2+} alone account for positive loading on the 4^{th} component with 8.67 % variance.

In the post-monsoon season; As, PO_4^{3-} and HCO_3^{-} account for positive loadings on PC1 with 36.87 % variance. Both As and PO_4^{3-} have similar anionic properties and therefore may remain adsorbed on similar substrates. Alkaline conditions could assist in the breakdown and dissolution of minerals and substrates which bind As and PO_4^{3-}, therefore leading to their co-evolution. Electrical conductivity, Mg^{2+}, H_4SiO_4 and TDS have positive loading on PC 2, while ORP has negative loading on the same component which has a variance of 15.43%. PC 2 is indicative of silicate weathering and dissolution. PC 3 is represented by high loading from K^{+} and Ca^{2+} with a variance of 10.15 %. Agricultural liming can increase the Ca^{2+} in groundwater, but it will have negligible effect on K^{+} availability; therefore liming is not the process affecting this component. Dissolution of minerals like polyhalite can release both K^{+} and Ca^{2+} in groundwater and can be the hydrochemical process affecting component 3. pH, DO, Na^{+} and H_4SiO_4 represent component 4 which has a variance 7.37%. This component represents infiltration of fresh surface water with higher DO as well as CO_2, which ultimately lead to silicate weathering and release of Na^{+}.

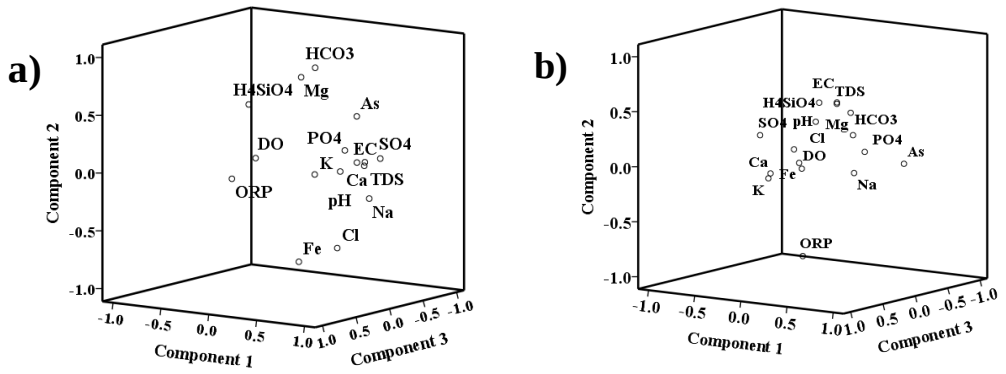

Figure 4.23: Loadings plots for the PCA with three components in (a) monsoon and (b) post-monsoon seasons respectively

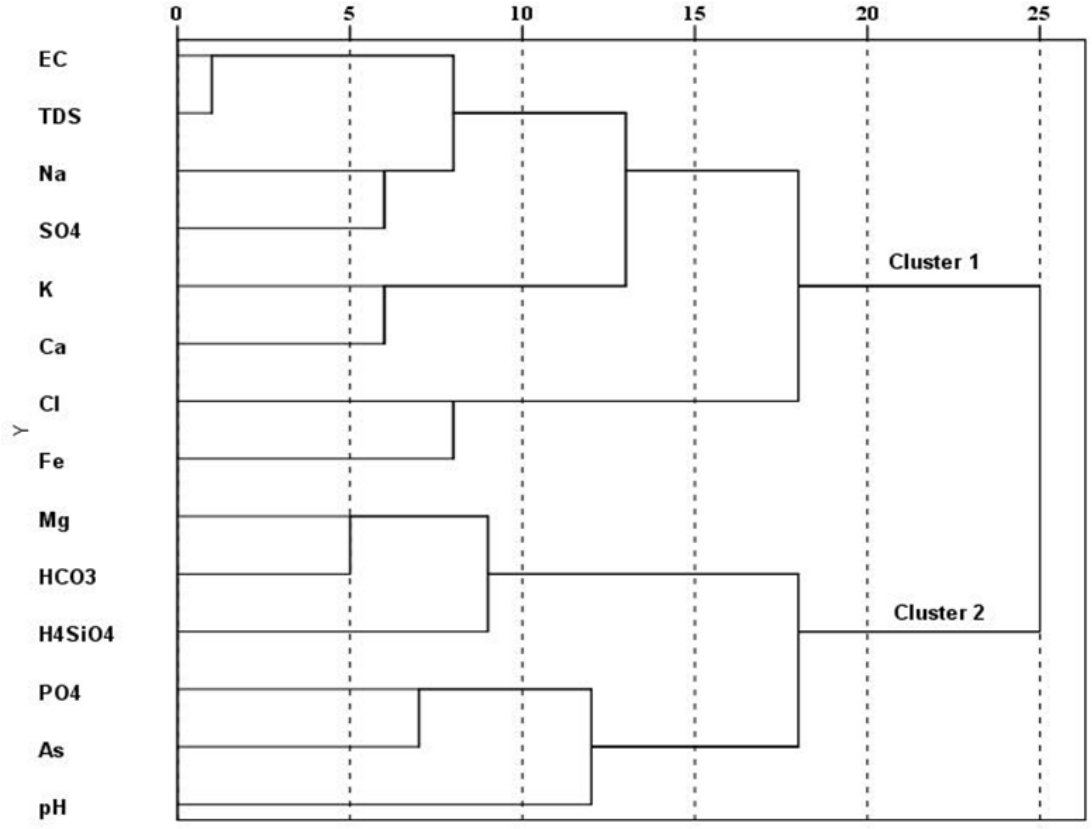

Figure 4.24: Dendrogram for hierarchical cluster analysis in the monsoon season

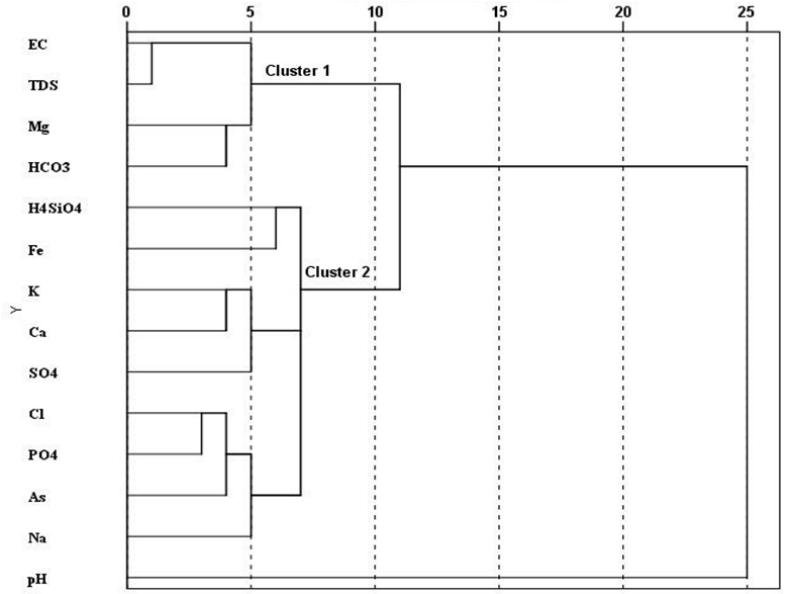

Figure 4.25: Dendrogram for hierarchical cluster analysis in the post-monsoon season

II. Hierarchical cluster analysis (HCA)

Hierarchical cluster analysis was performed on standardized groundwater data of monsoon and pre-monsoon. In both the monsoon as well as the post-monsoon seasons, weathering processes are dominant. In monsoon season, EC, TDS, Na^+, SO_4^{2-}, K^+ and Ca^{2+} are grouped together in cluster 1; dissolution of various minerals like gypsum, mirabilite and polyhalite could account for this trend (Fig. 4.24). Both silicate as well as carbonate weathering is associated with Mg as can be seen in cluster 2. Phosphate and As are clustered together (Fig. 4.24) and show a strong relationship because of the similarities between their anionic forms. Both As and PO_4^{3-} may be adsorbed on similar adsorption sites and released during the weathering and dissolution of these. The Jorhat district is an important tea-production zone of Assam which relies heavily on phosphate fertilizers like monoammonium phosphate (MAP) or monocalcium phosphate (MCP). The level of phosphate detected in the groundwater of the region is very low and it is unlikely that anthropogenic fertilizers could be the cause of this relationship. More over pH appears to have a control on the release of both PO_4^{3-} and As.

In the post-monsoon season it observed that most of the EC and TDS in the groundwater are contributed by carbonate weathering (Fig. 4.25). Silicate weathering in turn is associated with Fe in the system. This could be due to the fact that Fe remains adsorbed on sites provided by silicates, and weathering of silicates could lead to mobilization of Fe in the groundwater. Potassium, Ca^{2+} and SO_4^{2-} in cluster 2 (Fig. 4.25) could be released from various salts like gypsum, mirabilite and polyhalite due to weathering and dissolution effects of the precipitation. In the post-monsoon season also As and PO_4^{3-} are grouped together (Fig. 4.25), the reason could be similar to that in the monsoon.

4.3.3.6. Saturation indices

In our study, speciation modelling was performed on a set of 7 representative samples in both monsoon and post-monsoon seasons and it was observed that there was no major difference between the SI values for both the seasons. It was observed that the groundwater of the Jorhat district is under saturated with respect to various As phases like Arsenolite, As_2O_5, Claudetite and $FeAsO_4{:}_2H_2O$ (Table 4.15 and 4.16). Primary Fe minerals, like goethite, was not detected or was found to be under-saturated in most of the samples in both monsoon and post-monsoon seasons except in one sample each in monsoon (J1 04) and post-monsoon (J2 05) (Table 4.15 and 4.16). $Fe_2(SO_4)_3$ is especially under-saturated in both the seasons (Table 4.15 and 4.16). This indicates that the mineral has a tendency to undergo dissolution. The mineral $Fe_2(SO_4)_3$ may be formed as the result of pyrite oxidation. We have already discussed about the possible involvement of pyrite as a source of As in the previous sections. The fact that the As phases are under-saturated in both the seasons is alarming, as in the near future there is every possibility of an increase of the As levels in the groundwater. The pollution appears to be in its initial stages given the slow flowing nature of the groundwater, therefore the As level in the groundwater of Jorhat district will increase in the near future to develop into a full blown endemic condition observed in many districts of West Bengal in India and that in Bangladesh.

Table 4.15: Saturation indices of selected aqueous phases in the monsoon season calculated by using MINTEQ. NF here stands for 'not found'. am, c and s stand for amorphous, crystalline and solid respectively

	Samples						
Aqueous Phase	**J1-01**	**J1-04**	**J1-05**	**J1-7b**	**J1-11**	**J1-13**	**J1-21**
Aragonite	-1.18	-0.65	-1.43	-1.09	0.09	-0.58	0.26
Arsenolite	-12.38	-12.87	-19.75	-11.97	-12.27	-13.81	-12.70
As_2O_5	-38.12	-35.96	-31.28	-37.59	-34.08	-35.99	-34.89
Claudetite	-12.42	-12.91	-19.79	-12.01	-12.31	-13.85	-12.74
$Fe(OH)_2$ (am)	-4.52	-3.19	NF	-4.10	-2.85	-1.49	-2.50
$Fe(OH)_2$(c)	-3.92	-2.59	NF	-3.50	-2.25	-0.89	-1.90
Gypsum	-2.63	-2.55	-2.93	-2.89	-2.28	-3.05	-2.25
Halite	-7.60	-7.34	-7.56	-7.63	-7.09	-7.42	-7.08
Mirabilite	-8.16	-8.01	-8.46	-8.49	-7.39	-8.79	-7.33
Siderite	0.09	0.89	NF	0.17	0.72	1.63	0.86
$Fe(OH)_2.7Cl._3$(s)	NF	NF	8.16	NF	NF	NF	NF
$Fe_2(SO_4)_3$(s)	NF	NF	-32.26	NF	NF	NF	NF
$FeAsO_4$:$2H_2O$(s)	NF	NF	-4.70	NF	NF	NF	NF
Ferrihydrite	NF	NF	4.89	NF	NF	NF	NF
Ferrihydrite (aged)	NF	NF	5.40	NF	NF	NF	NF
Goethite	NF	NF	7.60	NF	NF	NF	NF

Table 4.16: Saturation indices of selected aqueous phases in the post-monsoon season calculated by using MINTEQ. NF here stands for 'not found'. am, c and s stand for amorphous, crystalline and solid respectively

	Samples						
Aqueous Phase	**J1-01**	**J1-01b**	**J2-04**	**J2-06**	**J2-09**	**J2-10**	**J2-11**
Aragonite	-1.53	-1.30	-1.30	-1.56	-1.74	-1.76	-0.73
Arsenolite	-11.99	-11.30	-17.97	-12.18	-12.33	-12.28	-10.95
As_2O_5	-32.12	-34.41	-31.25	-37.38	-32.99	-34.76	-32.24
Claudetite	-12.03	-11.34	-18.01	-12.22	-12.37	-12.32	-10.99
$Fe(OH)_2$ (am)	-4.38	-4.10	NF	-4.08	-4.04	-3.59	-4.17
$Fe(OH)_2$(c)	-3.78	-3.50	NF	-3.48	-3.44	-2.99	-3.57
Gypsum	-3.34	-3.32	-3.21	-2.96	-3.52	-3.42	-3.38
Halite	-7.63	-7.70	-7.43	-7.50	-7.66	-7.70	-7.31
Mirabilite	-8.78	-9.02	-8.59	-8.04	-9.08	-9.00	-8.39
Siderite	0.14	0.01	NF	-0.03	0.45	0.43	-0.19
$Fe(OH)_2.7Cl.3$(s)	NF	NF	8.68	NF	NF	NF	NF
$Fe_2(SO_4)_3$(s)	NF	NF	-32.95	NF	NF	NF	NF
$FeAsO_4:2H_2O$(s)	NF	NF	-4.13	NF	NF	NF	NF
Ferrihydrite	NF	NF	5.44	NF	NF	NF	NF
Ferrihydrite (aged)	NF	NF	5.95	NF	NF	NF	NF
Goethite	NF	NF	8.15	NF	NF	NF	NF

4.4. Conclusion and recommendation

Weathering and dissolution processes appear to control the overall hydrogeochemistry of the BFP region. Calcite and silicate weathering are the two most important processes in this regard. Overall the conditions in the BFP appear to be a mixture of reducing and oxidising conditions, although the former seems to dominate over the latter. This indicates the existence of a mixed aquifer system in the BFP. Arsenic and Fe showed a

high positive relation with each other both spatially and seasonally. The process of As release appears to be affected by alkalinity and pH increase. The above observation could be due to the prevalence of reductive dissolution of Fe (hydr)oxides in releasing As. Iron (hydr)oxides also appears to control the mobilization of F^- in the north bank to some extent. The possible mechanism could be the desorption of adsorbed F^- from Fe (hydr)oxides. Cluster analysis showed a similar result in the south bank as well. It was observed that both SO_4^{2-} and F^- were clustered close to As and Fe, and thus anions like F^- and SO_4^{2-} appear to be partially adsorbed on the Fe (hydr)oxide phase and later released under favourable conditions of pH and alkalinity. In the pre-monsoon season, F^- and SO_4^{2-} are also clustered together indicating the presence of desorptive processes in their release. The process of reductive dissolution Fe (hydr)oxide appears to be prevailing throughout the year as As and Fe were clustered together in both pre and post-monsoon seasons. Proximity to the river could play an important role in the distribution of both As and F^-. Newer alluvial sediments close to the river could have higher content of As bearing minerals as well as organic matter on account of their relatively un-oxidised state resulting in higher groundwater As closer to the river. Although F^- did not show any relation with river proximity, it appears that the alluvial conditions are not suitable for occurrence of F^- and higher F^- content would appear far from the flood plain region, in isolated pockets where recharge rates are very low. Another important observation was that high groundwater As do not appear to be a continuous phenomenon; the contaminant could originate in patches or in As hotspots from which recharge and mobilization could occur. Study of groundwater condition in the Jorhat district reveal that reductive hydrolysis of Fe (hydr)oxides process could be influenced by the local hydrogeochemistry. Anthropogenic processes could also play minor but important roles in modifying the trend of As release region wise. Sulphide oxidation could be one of the minor processes of As evolution in the Jorhat district. Monsoon sampling in Jorhat was conducted just at the onset of the first rains in the first week of June. Lower level of water saturation in the aquifers in pre-monsoon could mean a more oxidising condition suitable for incidences of sulphide oxidation. Also the use of phosphate fertilizers in the Jorhat region could be an important anthropogenic factor which could locally affect the As mobilization process in the district. Mineralogical studies of the sediments in the BFP show the presence of As minerals

like arsnopyrite and walpurgite. This indicates that mineral phases could be the primary sources of As in the region. Finally we can conclude that the primary source of As in the BFP could be the alluvial sediments with As bearing minerals, which are weathered and brought down from the Himalayan mountains by the Brahmaputra River and its tributaries.

This study could be improved further by the increasing the sampling density, as the number of samples collected was less. Influence of anthropogenic activities on As and F^- contamination can be studied by intensive and localized sampling in smaller regions of the BFP. In order to gain a better understanding of the role played by the river and fluvial environment in As and F^- contamination, comparative groundwater sampling should be carried out in regions lying outside the BFP, especially in arid regions which lack fluvial conditions. Isotope tracer techniques can be used for identifying groundwater As and F^- flow paths and recharge routes. Which in turn can be used for identifying As hotspots and F^- enriched aquifers. This can be helpful in delineating regions with safe levels of groundwater As and F^- for human consumption.

References

1. Harvey, C.F., Swartz, C.H., Badruzzaman, A.B.M., Blute, N.K., Yu, W., Ali, M.A., Jay, J., Beckie, R., Niedan, V., Brabander, D., Oates, P.M., Ashfaque, K.N., Islam, S., Hemond, H.F., Ahmed, M.F. Groundwater arsenic contamination on the Ganges Delta: biogeochemistry, hydrology, human perturbations, and human suffering on a large scale, *C.R. Geoscience*, **337** (1-2), 285-296, 2005.`
2. Liao, C., Lin, T., Chen, S. A Weibull-PBPK model for assessing risk of arsenic induced skin lesions in children, *Sci. Total Environ.* **392** (2-3), 203–217, 2008.
3. Halim, M.A., Majumder, R.K., Nessa, S.A., Hiroshiro, Y., Sasaki, K., Saha, B.B., Saepuloh, A., Jinno, K. Evaluation of processes controlling the geochemical constituents in deep groundwater in Bangladesh: Spatial variability on arsenic and boron enrichment, *Hazardous Mat.* **180** (1-3), 50-62, 2010.

4. Bundschuh, J., Bonorino, G., Viero, A.P., Albouy, R., Fuertes, A. Arsenic and other trace elements in sedimentary aquifers in the Chaco-Pampean Plain, Argentina: *31st INTERNATIONAL GEOL. CONG*., 2000, Rı´o de Janeiro, Brazil. 27–32.
5. Bundschuh, J., Farias, B., Martin, R., Storniolo, A., Bhattacharya, P., Cortes, J., G. Bonorino,. R Alboury. Grounwater arsenic in the Chaco-Pampean Plain, Argentina: case study from Robles County, Santiago del Estero Province, *Applied Geochemistry*, **19** (2), 231–243, 2004.
6. Smedley, P.L., & Kinniburgh, D.G. A review of the source, behavior and distribution of arsenic in natural waters, *Appl Geochem*, **17** (5), 517–568, 2002.
7. Bhattacharya, P., Frisbie, S.H., Smith, E., Naidu, R., Jacks, G., Sarkar, B., Arsenic in the environment: a global perspective, in *Handbook of Heavy Metals in the Environment,* Sarkar, B. (Ed.), Marcell Dekker Inc., New York. 2002a, 147–215.
8. Bhattacharyya, R., Jana, J., Nath, B., Sahu, S., Chatterjee, D., Jacks, G. Groundwater arsenic mobilization in the Bengal Delta Plain, the use of ferralite as a possible remedial measure-a case study, *Appl. Geochem*. **18** (9), 1435–1451, 2003.
9. Smedley, P.L., Nicolli, H.B., Macdonald, D.M.J., Barros, A.J., Tullio, J.O. Hydrogeochemistry of arsenic and other inorganic constituents in groundwaters from La Pampa, Argentina, *Appl. Geochem.* **17** (3), 259–284, 2002.
10. Smedley, P.L., Zhang, M., Zhang, G. and Luo, Z. Mobilisation of arsenic and other trace elements in fluvio-lacustrine aquifers of the Huhhot Basin, Inner Mongolia. *Appl Geochem*, **18** (9), 1453–1477, 2003.
11. Ben, D.S., Berner, Z., Chandrasekharam, D., Karmakar, J. Arsenic enrichment in groundwater of West Bengal, India: geochemical evidence for mobilization of As under reducing conditions, *Appl. Geochem.* **18** (9), 1417–1434, 2003.
12. Ahmed, K.M., Bhattacharya, P., Hasan, M.A., Akhter, S.H., Alam, S.M.M., Bhuyan, M.A.H., Imam, M.B., Khan, A.A., Sracek, O. Arsenic enrichment in groundwater of the alluvial aquifers in Bangladesh: an overview, *Appl. Geochem*. **19** (2), 181–200, 2004.

13. Kumar, Manish., Kumar, Pankaj., Ramanathan, A.L., Bhattacharya, Prosun., Thunvik, Roger., Singh, Umesh K., Tsujimura,M., Sracek, Ondra, Arsenic enrichment in groundwater in the middle Gangetic Plain of Ghazipur District in Uttar Pradesh, India, *J. Geochem. Explor.* **105** (3), 83–94, 2010.
14. Kumar, P., Kumar, M., Ramanathan, A.L., Tsujimura, M. Tracing the factors responsible for arsenic enrichment in groundwater of the middle GangeticPlain, India: a source identification perspective, *Environ Geochem Hlth.* **32** (2), 129–146, 2010.
15. Ghosh, N.C., & Singh, R.D. *Groundwater Arsenic Contamination in India: Vulnerability and Scope for Remedy*. NIH, Roorkee, 2009.
16. Guidelines for Drinking-Water Quality, 2nd edition WHO, Geneva, 1993.
17. Reddy, D.P. *Arsenic and Iron Contamination in Ground Water in Lower Brahmaputra Basin in Bongaigaon And Part Of Dhubri Districts Of Assam State, India*, India Water Week-Water, Energy and Food Security, 2012.
18. Singh, A.K. Arsenic Contamination in Groundwater of North Eastern India Published in *PROCEEDINGS OF NATIONAL SEMINAR ON HYDROLOGY WITH FOCAL THEME ON "WATER QUALITY*" 2004, held at National Institute of Hydrology, Roorkee.
19. Bhuyan. B., Bhuyan, D. Groundwater arsenic contamination status in Dhakuakhana sub-division of Lakhimpur district, Assam, India, *Acta Chimica & Pharmaceutica Indica,* **1** (1) 14-19, 2011.
20. Mukherjee, A., Sengupta, M.K., Hossain, M.A., Ahmed, S., Das, B., Nayak, B., Lodh, D., Rahman, M.M., Chakraborty, D. Arsenic Contamination in Groundwater: A Global Perspective with Emphasis on the Asian Scenario, *J Health Popul Nutr.* **24** (2), 142-163, 2006.
21. Bhattacharya, P., Chatterjee, D., Jacks, G. Occurrence of arsenic contamination of groundwater in alluvial aquifers from Delta Plain, Eastern India: option for safe drinking supply, *Int J Water Resour D*. **13** (1), 79–92, 1997.
22. Nickson,R., McArthur, J.M., Burgess, W., Ahmed, K.M., Ravenscroft, P., Rahman, M., Arsenic poisoning of Bangladesh groundwater, *Nature* **395**, 338, 1998.

23. Nickson, R.T., Mcarthur, J.M., Ravenscroft, P., Burgess, W.G., and Ahmed, K.M.. Mechanism of arsenic Release to Groundwater, Bangladesh and West Bengal. *Appl. Geochem*. **15** (4), 403-413, 1999.

24. McArthur, J.M., Ravenscroft, P., Safiullah, S., Thirlwall, M.F. Arsenic in groundwater: Testing pollution mechanisms for sedimentary aquifers in Bangladesh, *Water Resources Research*, **37** (1), 109-117, 2001.

25. Harvey, C., Swartz, C.H., Badruzzaman, A.B.M., Keon-Blute, N.E., Yu, W., Ashraf Ali, M., Jay, J., Beckie, R., Niedam, V., Brabander, D.J., Oates, P.M., Ashfaque, K.N., Islam, S., Hemond, H.F., Ahmed, M.F. Arsenic mobility and groundwater extraction in Bangladesh, *Science*, **298** (5598), 1602–1606, 2002.

26. Hoang, T.H., Bang, S., Kim, K.W., Nguyen, M.H., Dang, D. M. Arsenic in Groundwater and Sediment in the Mekong River Delta, Vietnam, *Environmental pollution*, **158** (8), 2648–2658, 2010.

27. Stumm, W. and Morgan, J.J. Aquatic Chemistry, 2nd edition, JohnWiley& Sons, NewYork, 1981.

28. K. Brindha., R. Rajesh., R. Murugan., L. Elango. Fluoride contamination in groundwater in parts of Nalgonda District, Andhra Pradesh, India, *Environ Monit Assess.* **172** (1-4), 481-92, 2010.

29. Brunt. R; Vasak. L; Griffioen. J. Fluoride in groundwater: Probability of excessive concentration on global scale, *INTERNATIONAL GROUNDWATER RESOURCES ASSESSMENT CENTER (IGRAC)*, 2004.

30. Pillai, K.S., & Stanley, V.A. Implications of fluoride-an endless uncertainty, *J Environ Biol*, **23** (1), 81–87, 2002.

31. Susheela, A. K. *A Treatise on Fluorosis*, Fluorosis Research and Rural Development Foundation, Delhi, 2001.

32. Chakraborti, D., Chanda, C.R., Samanta, G., Chowdhury, U.K., Mukherjee, S.C., Pal, A.B., Sharma, B., Mahanta, K.J., Ahmed, H.A., Sing, B. Fluorosis in Assam – India. *Current Science*, **78** (12), 1421-1423, 2000.

33. Das, B., Talukdar, J., Sarma, S., Gohain, B., Dutta, R.K., Das, H.B., Das, S.C. Fluoride and other inorganic constituents in groundwater of Guwahati, Assam, India, *Current Science*, **85** (5) 657-661, 2003.

34. Saxena, V.K., & Ahmed, S. Dissolution of fluoride in groundwater: a water-rock interaction study, *Environmental Geology*, **40** (9), 1084-1087, 2001.

35. Saxena, V.K., & Ahmed S. Inferring the chemical parameters for the dissolution of fluoride in groundwater, *Environmental Geology*, **43** (6), 731–736, 2002.

36. Arveti, N., Sarma. MR., Aitkenhead-Peterson, J.A., Sunil, K. Fluoride incidence in groundwater: a case study from Talupula, Andhra Pradesh, India, *Environ Monit Assess*, **172** (1-4), 427-443, 2010.

37. Jain, K.S., Agarwal, P.K., Singh, V.P. *Hydrology and Water Resources of India*, Water Sci and Technology Library. Springer, **57**, 2007, 419-472.

38. Domenico P. A. *Concepts and models in groundwater hydrology*. McGrawHill, New York, 1972.

39. Wallick E. I., Toth J. Methods of regional groundwater flow analysis with suggestions for the use of environmental isotope, in *Interpretation of Environmental Isotope and Hydrochemical Data in Groundwater Hydrology*. IAEA, 1976, Vienna, 37–64.

40. Toth J. The role of regional gravity flow in the chemical and thermal evolution of groundwater, in *PROCEEDINGS OF THE 1ST CANADIAN/AMERICAN CONFERENCE ON HYDROGEOLOGY*, 1984, Banff, Alberta.

41. Kumar, M., Ramanathan, A.L., Rao, M. S., Kumar, B. Identification and evaluation of hydrogeochemical processes in the groundwater environment of Delhi, *India, Environ. Geol.* **50** (7), 1025–1039, 2006.

42. Piper A.M. A graphic procedure in the chemical interpretation of water analysis. US Geol Surv Groundwater Note 12, 1953.

43. Gibbs R. J. Mechanism controlling world water chemistry. *Science*, **170** (3962), 1088–1090, 1970.

44. Stallard R. F. & Edmond J. M. Geochemistry of the Amazon, the influence of geology and weathering environment on the dissolved load, *Journal of Geophysical Research*, **88** (C14), 9671–9688, 1983.

45. Meybeck, M. Global chemical weathering of surficial rocks estimated from river-dissolved leads, *American Journal of Science*, **287** (5), 401–428, 1987.

46. Sarin, M. M., Krishnaswmay, S., Dilli, K., Somayajulu, B. L. K., Moore, W. S. Major ion chemistry of the Ganga-Brahmaputra river system: Weathering

processes and fluxes to the Bay of Bengal, *Geochimica et Cosmochimica Acta.* **53** (5), 997–1009, 1989.

47. Mackenzie F.J, Garrells R.H. Silicates: reactivity with water, *Sci J* **1505** 57–58 1965.
48. Rajmohan, N, Elango L. Identification and evolution of hydrogeochemical processes in the groundwater environment in an area of the Palar and Cheyyar River Basins, Southern India. *Environ Geol,* **46** (1), 47–61, 2004.
49. Kumar, M., Kumari, K., Singh, U.K., Ramanathan, A.L. Hydrogeochemical processes in the groundwater environment of Muktsar, Punjab: conventional graphical and multivariate statistical approach, *Environ Geol.* **57** (4), 873-884, 2008.
50. Wu. W., Xu, S., Yang, J., Yin, H. Silicate weathering and CO_2 consumption deduced from the seven Chinese rivers originating in the Quinghai-Tibet Plateau, *Chemical Geology*, **249** (3-4), 307-320, 2008.
51. Maya A, L., Loucks, M. D. Solute and isotopic geochemistry and groundwater flow in the Central Wasatch Range, Utah, *J Hydrol.* **172** (1-4), 31–59, 1995.
52. Cerling, T.E., Pederson, B.L., Damm, K.L.V. Sodium–calcium ion exchange in the weathering of shales: implications for global weathering budgets, *Geology*, **17** (6), 552–554, 1989.
53. Fisher, R.S., Mulican, W.F. III. Hydrochemical evolution of sodium–sulphate and sodium–chloride groundwater beneath the Northern Chihuahuan desert, Trans-Pecos, Texas, USA, *Hydrogeol. J.* **10** (4), 455–474, 1997.
54. Reddy, A.G.S., Reddy, D.V., Rao, P.N. and Prasad Maruthy K. Hydrogeochemical characterization of fluoride rich groundwater of Wailpalli watershed, Nalgonda District, Andhra Pradesh, India, *Environ Monit Assess.* **171** (1-4), 561-577, 2010.
55. Garrels R.M., & Mackenzie F.T *Evolution of sedimentary rocks*. WW Norton, New York, 1971.
56. Das, B.K., Kaur, P. Major ion chemistry of Renuka lake and weathering processes, Sirmaur district, Himachal Pradesh, India, *Envion Geol.* **40** (7), 908–917, 2001.

57. Kim, S.H., Kim, K., Ko, K.S., Kim, Y., Lee, K.S. Co-Contamination of Arsenic and Fluoride in the Groundwater of Unconsolidated Aquifers under Reducing Environments, *Chemosphere*, **87** (8), 851–856, 2012.

58. Vencelides, Z., Sracek, O., & Prommer, H. 2007. Modelling of iron cycling and its impact on the electron balance at a petroleum hydrocarbon contaminated site in Hnevice, Czech Republic, *Journal of Contaminant Hydrology*, **89** (3-4), 270–294 2007.

59. Armienta, M., Segovia, N. Arsenic and Fluoride in the Groundwater of Mexico. *Environmental geochemistry and health*, **30** (4), 345–353, 2008.

60. Durov S. A. Natural waters and graphical representation of their composition, *Dokl Akad Nauk USSR* **59**, 87–90 1948.

61. Schoeller. Hydrodynamique lans lekarst (ecoulemented emmagusinement). *Actes Colloques Doubronik,* I, AIHS et UNESCO, 3–20, 1965.

62. Reddy, A.G.S., & Kumar, K.N. Identification of the hydrogeochemical processes in groundwater using major ion chemistry: A case study of Penna-Chitravathi river basins in Southern India, *Environ Monit Assess*, **170** (1-4), 365-382, 2010.

63. Subramani, T., Rajmohan. N., Elango. L. Groundwater geochemistry and identification of hydrogeochemical processes in a hard rock region, Southern India, *Environ Monit Assess*, **162** (1-4), 123-137, 2010.

64. Jankowski J., & Acworth R. I. Impact of debris-flow deposits on hydrogeochemical processes and the development of dryland salinity in the Yass River catchment, New South Wales, Australia, *Hydrogeol J.* **5** (4),71–88, 1997.

65. Mukherjee, A., Brömssen, M. V., Scanlon, B. R., Bhattacharya, P., Fryar, A. E., Hasan, M. A., Ahmed, K. M., Chatterjee, D., Jacks, G., Sracek, O. Hydrogeochemical Comparison and Effects of Overlapping Redox Zones on Groundwater Arsenic near the Western (Bhagirathi Sub-Basin, India) and Eastern (Meghna Sub-Basin, Bangladesh) Margins of the Bengal Basin, *Journal of contaminant hydrology*, **99** (1-4), 31–48, 2008.

66. Davenport, J. R., & Peryea, F. J. Phosphate fertilizers influence leaching of lead and arsenic in a soil contaminated with lead arsenate, *Water, Air, and Soil Pollution*, **57-58**, (1), 101-110, 1991.

67. Farooqi, A., Masuda, H., Firdous, N. Toxic fluoride and arsenic contaminated groundwater in the Lahore and Kasur districts, Punjab, Pakistan and possible contaminant sources, *Environ. Pollut.* **145** (3), 839–849, 2007.

68. Ground Water Information Booklet, Jorhat District, *Central Ground Waterboard, 2008.*